Faculty of Electrical Technology and Engineering

TRANSFER TORQUE ANALYSIS OF MAGNETIC GEAR USING FINAL ELEMENT FOR EV APPLICATION

MUHAMMAD ADIB BIN SHAFEE

Bachelor of Electrical Engineering Technology (Industrial Power) with Honours

2024

TRANSFER TORQUE ANALYSIS OF MAGNETIC GEAR USING FINAL ELEMENT FOR EV APPLICATION

MUHAMMAD ADIB BIN SHAFEE

**A project report submitted
in partial fulfillment of the requirements for the degree of
Bachelor of Electrical Engineering Technology (Industrial Power) with Honours**

Faculty of Electrical Technology and Engineering

UNIVERSITI TEKNIKAL MALAYSIA MELAKA

2024

DECLARATION

I declare that this project report entitled “Transfer Torque Analysis of Magnetic Gear Using Final Element for EV Application” is the result of my own research except as cited in the references. The project report has not been accepted for any degree and is not concurrently submitted in candidature of any other degree.

Signature : ....

Student Name : Muhammad Adib Bin Shafee

Date : 3 January 2025

UNIVERSITI TEKNIKAL MALAYSIA MELAKA

APPROVAL

I hereby declare that I have checked this project report and in my opinion, this project report is adequate in terms of scope and quality for the award of the degree of Bachelor of Electrical Engineering Technology (Industrial Power) with Honours.

Signature :

Supervisor Name : Ts. Dr. Mohd Firdaus Bin Mohd Ab Halim

Date : 24 January 2025

Signature :

Co-Supervisor Name (if any) :

Date :

UNIVERSITI TEKNIKAL MALAYSIA MELAKA

DEDICATION

To This study is dedicated to my beloved parents, who have been our source of inspiration, guide and give me strength, when I thought of giving up, who continually provide their moral, spiritual, emotional and financial support.

To my friends who become my supporter and help me to any problem I faced. The encourage me to finish this important research in time. They also give me inspiration message every time.

To my supervisor who believed that I will finish this research in time, helping me to make my research better, to inspire me to their inspiration stories when they are students before.

And lastly, I dedicated this report to my Mighty God that guides me, give strength, power of mind, protection and skills. All of this, I offer to you

UTeM
اونيۆرسيتي تيكنيكل مليسيا ملاك
UNIVERSITI TEKNIKAL MALAYSIA MELAKA

ABSTRACT

Although mechanical gear offers a high torque over volume ratio, it has inherent issues with heat, noise, vibration, and reliability. In recent years, magnetic gears (MG) and magnetically geared machines have been developed as a viable and workable substitute for traditional mechanical gearboxes in order to address the disadvantage of mechanical gears. In Concentric Magnetic Gear, (CMG), the number of pole pairs significantly influences the torque behavior of magnetic gears, yet comprehensive studies on the effects of various pole pair combinations remain limited. This information gap hinders the optimization of CMG designs, particularly for electric vehicle (EV) applications. Critical considerations such as gear ratio, torque ripple, and the relationship between inner and outer torque require further investigation to enhance the torque performance of EV systems. This study leverages JMAG software to analyze the transfer torque and optimize magnetic gear performance, focusing on minimizing torque ripple and maximizing average torque through various pole pair configurations. The research contributes to Sustainable Development Goals (SDGs) 7 (Affordable and Clean Energy) and 9 (Industry, Innovation, and Infrastructure) by advancing magnetic gear technology, reducing power losses, and improving energy efficiency in EVs. The findings support environmentally friendly transportation solutions and sustainable industrial growth, fostering innovative engineering practices. The objectives include design several model of the magnetic gear structure with various pole pair combinations using flux modulation principles and conduct a thorough evaluation of the torque behavior of Concentric Magnetic Gears using Finite Element Method (FEM) on several design pole pair. This work lays comparison all combination in term of torque ripple and the highest average torque also identifying configurations with optimal torque characteristics.

ABSTRAK

Walaupun gear mekanikal menawarkan tork yang tinggi berbanding nisbah isipadu, ia mempunyai masalah yang wujud dengan haba, bunyi, getaran dan kebolehpercayaan. Dalam tahun-tahun kebelakangan ini, Gear Magnetik (MG) dan mesin bergear magnet telah dibangunkan sebagai pengganti yang berdaya maju dan boleh digunakan untuk kotak gear mekanikal tradisional untuk menangani kelemahan gear mekanikal. Dalam *Concentric Magnetic Gear* (CMG), bilangan pasangan kutub mempengaruhi tingkah laku tork gear magnet dengan ketara, namun kajian menyeluruh tentang kesan pelbagai kombinasi pasangan kutub kekal terhad. Jurang maklumat ini menghalang pengoptimuman reka bentuk CMG, terutamanya untuk aplikasi kenderaan elektrik (EV). Pertimbangan kritikal seperti nisbah gear, riak tork, dan hubungan antara tork dalam dan luar memerlukan penyiasatan lanjut untuk meningkatkan prestasi tork sistem EV. Kajian ini memanfaatkan perisian JMAG untuk menganalisis tork pemindahan dan mengoptimumkan prestasi gear magnetik, memfokuskan pada meminimumkan riak tork dan memaksimumkan purata tork melalui pelbagai konfigurasi pasangan kutub. Penemuan ini menyokong penyelesaian pengangkutan mesra alam dan pertumbuhan industri yang mampan, memupuk amalan kejuruteraan yang inovatif. Objektifnya termasuk mereka bentuk beberapa model struktur gear magnet dengan pelbagai kombinasi pasangan kutub menggunakan prinsip modulasi fluks dan menjalankan penilaian menyeluruh terhadap tingkah laku tork *Concentric Magnetic Gears* (CMG) menggunakan *Finite Element Method* (FEM) pada beberapa pasangan kutub reka bentuk. Kerja ini meletakkan perbandingan semua kombinasi dari segi riak tork dan purata tork tertinggi serta mengenal pasti konfigurasi dengan ciri tork optimum.

ACKNOWLEDGEMENTS

First and foremost, I would like to express my gratitude to my supervisor, Ts. Dr. Mohd Firdaus Bin Mohd Ab Halim and co-supervisor for their precious guidance, words of wisdom and patient throughout this project.

I am also indebted to Universiti Teknikal Malaysia Melaka (UTeM) and Ts. Dr. Mohd Firdaus Bin Mohd Ab Halim for the financial support through funds which enables me to accomplish the project. Not forgetting my fellow colleague for the willingness of sharing his thoughts and ideas regarding the project.

My highest appreciation goes to my parents and family members for their love and prayer during the period of my study. An honourable mention also goes to my supervisor for all the motivation and understanding. And to my close friends, thank you for your cooperation.

Finally, I would like to thank all the staffs at the Universiti Teknikal Malaysia Melaka (UTeM), fellow colleagues and classmates, the faculty members, as well as other individuals who are not listed here for being co-operative and helpful.

UNIVERSITI TEKNIKAL MALAYSIA MELAKA

TABLE OF CONTENTS

UNIVERSITI TEKNIKAL MALAYSIA MELAKA

UNIVERSITI TEKNIKAL MALAYSIA MELAKA

LIST OF TABLES

UNIVERSITI TEKNIKAL MALAYSIA MELAKA

LIST OF FIGURES

UNIVERSITI TEKNIKAL MALAYSIA MELAKA

UNIVERSITI TEKNIKAL MALAYSIA MELAKA

LIST OF SYMBOLS

ℓ	-	Liter

اونيۈرسيتي تيكنيكل مليسيا ملاك
UNIVERSITI TEKNIKAL MALAYSIA MELAKA

LIST OF ABBREVIATIONS

EV	-	Electric Vehicle
CMG	-	Concentric Magnetic Gear
FEM	-	Finite Element Method
MG	-	Magnetic Gear
G_r	-	Gear Ratio
PM	-	Permenant Magnet
PMG	-	Planetary Magnetic Gear
HMG	-	Harmonic Magnetic Gear
FFT	-	Fast Fourier Transform
RAP	-	Radial Anisotropic Pattern
CAP	-	Circumferential Anisotropic Pattern
PCD	-	Parallel Pattern Circular Direction
PRD	-	Parallel Pattern Radial Direction
VTD	-	Volumetric Torque Density

اونيۏرسيتي تيكنيكل مليسيا ملاك
UNIVERSITI TEKNIKAL MALAYSIA MELAKA

LIST OF APPENDICES

UNIVERSITI TEKNIKAL MALAYSIA MELAKA

CHAPTER 1

INTRODUCTION

1.1 Background

Analyzing the transfer torque of magnetic gears using JMAG software for electric vehicle (EV) applications is a fascinating field. Because they have the potential to be more efficient than mechanical gears and are smaller and require less maintenance, magnetic gears are becoming more and more popular in electric vehicles (EV). JMAG software is an effective tool for modelling electromagnetic apparatus, which makes it a good choice for studying magnetic gears.

1.2 Addressing Critical Societal and Global Challenges Through Magnetic Gear

Analyzing the transfer torque of magnetic gears for electric vehicle (EV) applications using JMAG software addresses critical societal and global challenges by advancing sustainable transportation solutions. It lowers greenhouse gas emissions, conserves energy, and encourages the incorporation of renewable energy sources into the transportation sector by increasing the efficiency of EV components like magnetic gears. By generating skilled employment possibilities in high-tech businesses, this invention promotes technical competitiveness, propels the electrification of automobiles, and boosts economic growth. In the end, magnetic gear technology optimisation using cutting-edge modelling tools not only improves electric propulsion system performance but also speeds up the shift to a more robust and sustainable transportation infrastructure.

1.3 Problem Statement

Although mechanical gear offers a high torque over volume ratio, it has inherent issues with heat, noise, vibration, and reliability. In recent years, magnetic gears (MG) and magnetically geared machines have been developed as a viable and workable substitute for traditional mechanical gearboxes in order to address the disadvantage of mechanical gears.

The number of pole pairs affects the torque behaviour of magnetic gear. Comprehensive studies on the effects of various pole pair combinations on torque characteristics are still lacking. The optimisation of Concentric Magnetic Gear designs for particular applications, like electric cars, is hampered by this information gap.

One important consideration while evaluating Concentric Magnetic Gear for use in electric vehicle applications is their gear ratio. There is currently little information available about how inner and exterior torques affect the gear ratio. More research is necessary to optimise the gear ratio in EVs for better overall performance.

In motor applications, torque ripple is a crucial factor that impacts the system's efficiency and smoothness. It is still unknown how torque ripple varies with different combinations of pole pairs, particularly when flux modulation concepts are applied.

The use of electric vehicles (EVs) is essential to lowering carbon emissions and reliance on fossil fuels. In order to maximise torque efficiency and reduce power losses, this study uses JMAG software to analyse the transfer torque of magnetic gears in EVs. The study contributes to SDG 7: Affordable and Clean Energy and SDG 9: Industry, Innovation, and Infrastructure by improving magnetic gear systems, which encourages environmentally friendly transportation and creative engineering solutions.

UNIVERSITI TEKNIKAL MALAYSIA MELAKA

By improving transportation energy efficiency, the JMAG software analysis of transfer torque in magnetic gears for electric vehicle (EV) applications directly contributes to SDG 7. This research guarantees that EVs utilise less energy, increasing their efficiency and sustainability, by minimising power losses in these cars. Enhancing EV performance also contributes to the creation of greener modes of mobility, which is in line with the objective of ensuring that everyone has access to contemporary, cheap, dependable, and sustainable energy. This development contributes to a more sustainable energy future by lowering the environmental effect of transportation and encouraging the use of electric vehicles.

JMAG software's application in the optimisation of magnetic gears in electric vehicles (EVs) is an important technical breakthrough that promotes industrial growth and technological advancements two major pillars of SDG 9. This research contributes to resilient and sustainable industrialization by increasing the efficiency of EVs and fostering the growth of sustainable infrastructure and industries. The advancements in magnetic gear technology foster sustainable growth and innovation by providing a solid basis for future industrial practices. This promotes economic growth and guarantees that industrial development aligns with the objectives of environmental sustainability.

1.4 Project Objective

The main aim of the project objective is to conduct a thorough analysis of the transfer torque and efficiency of magnetic gears intended for electric vehicle (EV) applications using JMAG software. Specifically, the objectives are as follows:

a) To design several model of the magnetic gear structure with various pole pair combinations using flux modulation principles.

b) To conduct a thorough evaluation of the torque behavior of Concentric Magnetic Gears using Finite Element Method (FEM) on several design pole pair.

c) To compare all combination in term of torque ripple and the highest average torque.

UNIVERSITI TEKNIKAL MALAYSIA MELAKA

1.5 Scope of Project

The scope of this project are as follows:

a) The magnetic gear in this design has a diameter measuring 100mm up to 120mm, ensuring a compact yet efficient configuration suitable for various applications.

b) The specific type of magnetic gear chosen for this application is the Concentric Magnetic Gear (CMG). This selection offers several advantages, including compactness, high torque density, and reduced mechanical complexity, making it well-suited for various engineering and industrial applications requiring precise torque transmission.

c) The materials used in the Concentric Magnetic Gear are Nippon Steel (35H210) for the rotor and Neodymium Iron Boron (NdFeB_Br=1.2(T)) for the permanent magnets.

d) The model and design process exclusively relies on the utilization of JMAG-Designer18.1 software only, with no physical hardware involved in the assessment or implementation stages.

UNIVERSITI TEKNIKAL MALAYSIA MELAKA

CHAPTER 2

LITERATURE REVIEW

2.1 Introduction

Literature reviews this project will be included in this chapter. The case study of the project that may be developed to solve the issue is included in the literature research, along with the ability to understand the essential project's principles.

2.2 Magnetic Gear Topologies

According to Figure 2.1, the *concentric*, *harmonic*, and *planetary* magnetic gear topologies are the most important among the recently suggested MG topologies. The Concentric Magnetic Gear's high torque capabilities was first made public by Atallah et alin in 2001, notwithstanding the possibility that it originated with a Martin patent. The ferromagnetic pole-pieces positioned between the inner and outer PM rotors regulate the magnetic field in such a way that each rotor "sees" a working space harmonic that corresponds to its own number of poles. This is the fundamental principle of functioning of a concentric MG [1].

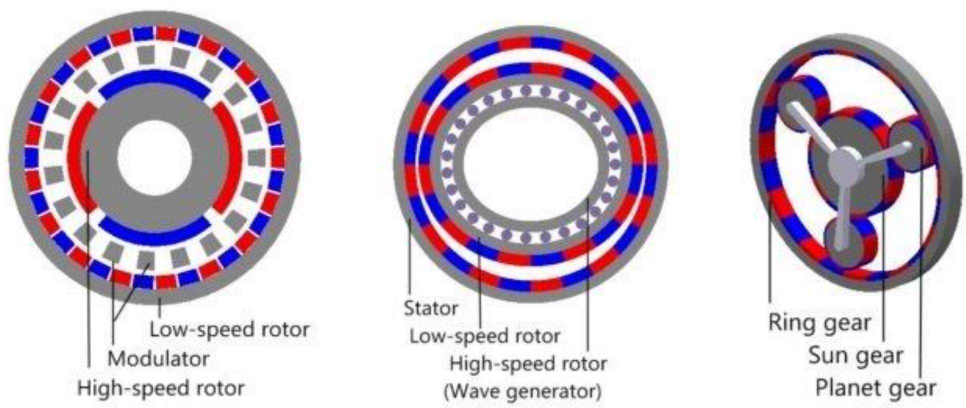

Figure 2.1: Concentric, Harmonic and Planetary Magnetic Gears [1]

The number of pole-pairs on the inner high-speed and outer low-speed rotors, *ph* and *pl*, and the number of modulator segments, *qm* are related by [1]:

$$qm = ph + pl \tag{1}$$

With a stationary modulator, the gear ratio G_r is given by [1]:

$$G_r = \frac{Pl}{Ph} = \frac{q_m - P_h}{P_h} = \frac{q_m}{P_h} - 1 = -\frac{\omega_h}{\omega_l} \tag{2}$$

Where ω_h and ω_l represent the rotors' relative angular speeds at high and low speeds. The two rotors' opposing rotational directions are indicated by the negative symbol. The gear ratio between the revolving modulator and high speed rotor, assuming the outer rotor remains stationary, is [1]:

$$G_r = \frac{q_m}{p_h} = \frac{\omega_h}{\omega_m} \tag{3}$$

2.2.1 Harmonic Magnetic Gears

Torque densities in the 150kNm/m^3 range have been highly promising for the harmonic gear. Although it is appealing because to its torque density, high gear ratios, and seamless torque transfer, it is difficult to build and depends on a low-speed, flexible rotor to create a sinusoidal change in the magnetic field that varies over time in the air gap between the rotors. A harmonic gear's gear ratio is expressed as [2]

UNIVERSITI TEKNIKAL MALAYSIA MELAKA

$$G_r = \frac{(-1)^{(k+1)} p_w}{p_1} \tag{4}$$

Where *k* stands for the numerous asynchronous space harmonics that are connected to each harmonic of the magnetic field generated by the PMs, and P_1 and P_2 stand for the number of poles on the low-speed rotor and the number of sinusoidal cycles between the low-speed rotor and stator, respectively [3].

In addition to the contactless benefits and no maintenance needs of MG, the MPG presented by Cheng-Chi Huang et al. delivers torque densities of over 100 kNm/m3. It functions similarly to a conventional mechanical planetary gear. The gearing ratio of it is established by [2]

$$G_r = \frac{P_r}{(P_s+P_r)} \tag{5}$$

where P_1 and P_2 are the pole pairs on the magnetic ring gear and sun gear, respectively with the pole-pair relationship on the planetary gear determined by [2]:

$$p_p = \frac{(p_1-p_s)}{2} \tag{6}$$

The MPG is more complicated than the concentric design, but it can achieve large torque densities and gearing ratios, just like the harmonic gear. Furthermore, not all magnetic material is used while transmitting torque .

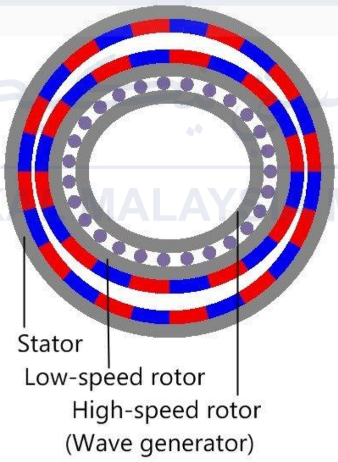

Figure 2.2: Harmonic Magnetic Gear [1]

2.2.2 Planetary Magnetic Gears

Planetary Magnetic Gear (PMG) consists of 4 main parts, ring gear, sun gear, planet gear attach to the carrier. All the gears can be set as output while the remaining gears act as the driving gear [4]. Torque transfer happened only when the two-driving gear are set correctly. The gear speed relationship is [5]:

$$W_p = \frac{P_s}{P_s+P_r}W_s + \frac{P_r}{P_s+P_r}W_r \tag{7}$$

Where Ps, Pr, ws, wr, and wp stand for the pole pairs for the ring gear, sun gear, carrier, and rotational velocity of the ring gear, respectively. Despite claims of a torque density of up to 100kNm/m^3, this design need two driving forces that are the same in order to generate torque at the output shaft. This is the reason why there haven't been many publications or updates about this topology [5][6].

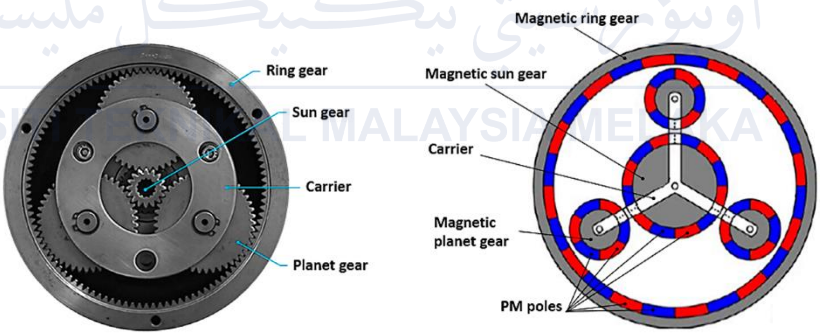

Figure 2.3: Planetary Magnetic Gear [3]

2.2.3 Concentric Magnetic Gears

The coaxial magnetic gear (CMG), a high-performance MG proposed by Atallah and Howe in 2001, operated on the basis of magnetic modulation generated by two PM rotors with the use of ferromagnetic components. The CMG has a higher torque density than the original MGs since all of the PMs contribute to torque gearbox at the same time[4]. Several enhanced CMG topologies were developed based on the field modulation theory in order to further increase efficiency. A high-speed outer rotor PM brushless machine and the CMG may be skillfully combined from the perspective of the coaxial structure to create a composite electrical machine known as the magnetic-geared permanent-magnet (MGPM) machine[7]. High torque density and low speed/high torque driving are both possible with the MGPM. This device has also drawn a lot of interest for applications including direct-drive electric vehicles and wind power generation. This study uses the ANSYS Maxwell package, the Finite Element Method (FEM), and the Fast Fourier Transform (FFT) to describe the working concept of CMG [7]. This indicates that FEM is used to acquire the flux density waves in both gaps, while FFT is used to obtain its harmonic spectra. Its behaviour may be explained by the modulation phenomena, which is essentially explained by the FFT. The cogging torque on the inner and outer gaps is determined using a movement band and a step-by-step FEM approach [8].

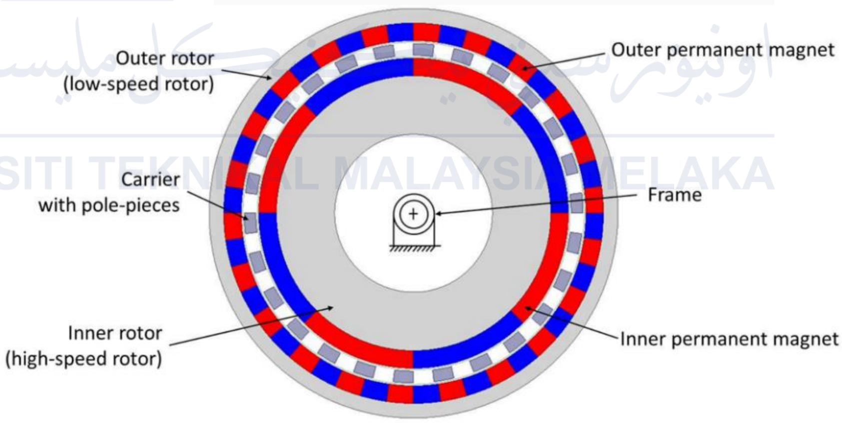

Figure 2.4: Concentric Magnetic Gear [8]

As seen in Figure 2.4, the CMG is made up of three main parts: an outer rotor that operates at a lower speed and has 44 permanent magnets that form 22 pole-pairs (Pout = 22), an inner rotor that operates at a higher speed and has 8 permanent magnets that form 4 pole-pairs (Pin = 4), and a magnetic steel modulator that is positioned between the two rotors and generates a square-wave modulation function with 26 pole pieces (Np = 26) [7].

The following summarises the connection between the aforementioned variables [9][10]:

$$P_{in} + P_{out} = N_p \quad [8][10]$$

where, for each rotor, P_{in}represents its inner, P_{out}its outer, and $N_p$its modulator speed [9]. There will be a consistent gear ratio between the other two portions of the gear while one of its three components is immobile. When the modulators are stationary, for instance ($N_p = 0$), The definition of the gear ratio between the inner and outer rotors is [11][12]:

$$G_r = \frac{p_{out}}{p_{in}} \quad [9][10]$$

and the direction of rotation of the rotors is opposite. By using the Maxwell Stress Tensor (MST), the electromagnetic torque that develops on the inner and outer rotors may be determined [13].

2.2.4 Pattern Setup for CMG

In Concentric Magnetic Gear (CMG), there are four distinct patterns, namely Radial Anisotropic Pattern (RAP), Circumferential Anisotropic Pattern (CAP), Parallel Pattern Circular Direction (PCD) and Parallel Pattern Radial Direction (PRD). Each of these patterns serves different functions within the context of condition monitoring [14].

UNIVERSITI TEKNIKAL MALAYSIA MELAKA

2.2.4.1 Radial Anisotropic Pattern (RAP)

The pattern and direction of radial anisotropic magnetization are depicted in Figure 2.5. Throughout the material, the magnetising vectors are made to assume radial shapes such as circles or cylinders by this magnetization pattern. The pattern in the CMG structure points towards the direction of the machine's centre [14].

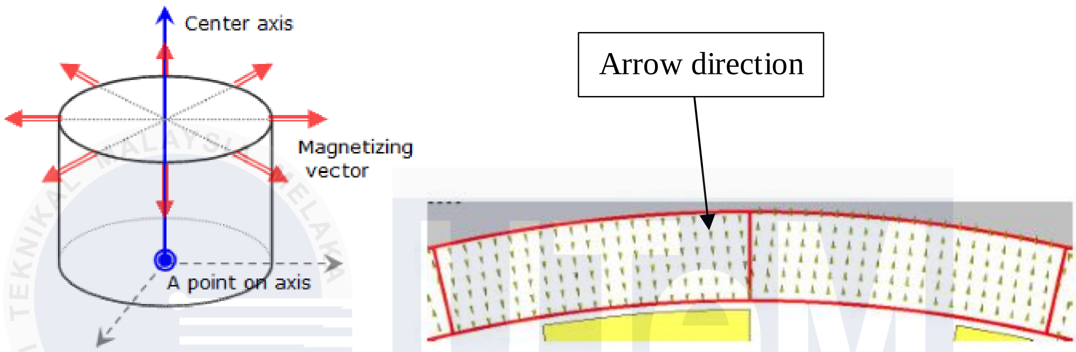

Figure 2.5: Radial Anisotropic Pattern (RAP) [14]

2.2.4.2 Circumferential Anisotropic Pattern (CAP)

The pattern and direction of circumferential anisotropic magnetization are depicted in Figure 2.6. The magnetization pattern assumes circles or cylinders across the material by setting the magnetising vectors in a circumferential orientation. The pattern in the CMG structure points either clockwise or anticlockwise in the direction of the nearby magnet [14].

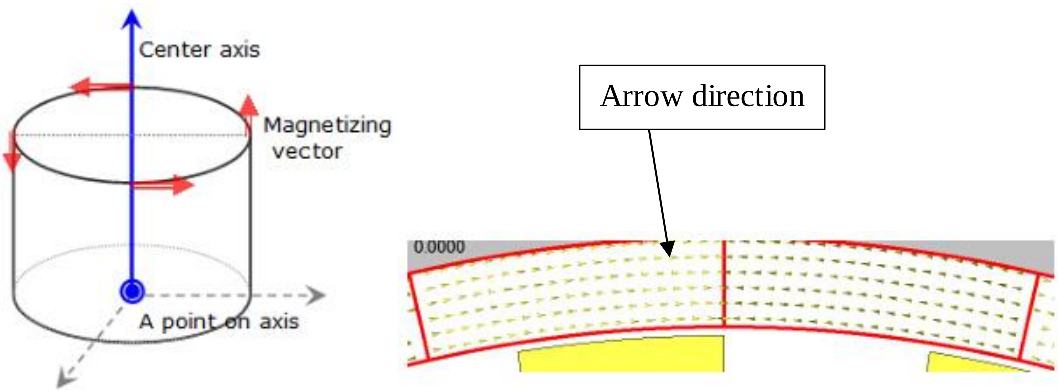

Figure 2.6: Circumferential Anisatropic Pattern (CAP) [14]

UNIVERSITI TEKNIKAL MALAYSIA MELAKA

2.2.4.3 Parallel Pattern Circular Direction

The parallel pattern's circular pattern and orientation are seen in Figure 2.7. The pole with the parallel magnetising vector repeats and reverses itself in the circumferential direction to form this magnetization pattern. The direction of every pattern in the CMG structure is parallel to the beginning flux line [14].

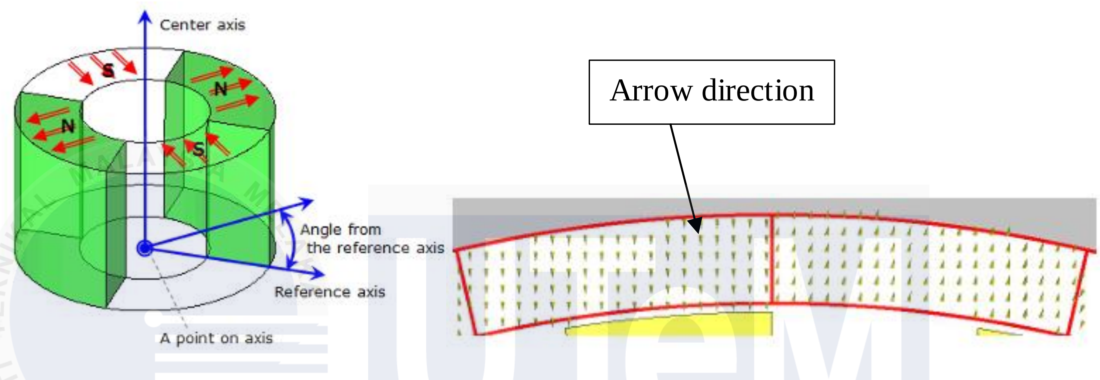

Figure 2.7: Parallel Pattern Circular Direction (PCD) [14]

2.2.4.4 Parallel Pattern Radial Direction (PRD)

The parallel pattern's radial pattern and direction are seen in Figure 2.8. The pole with the magnetising vector in the radial direction repeats and reverses itself in the circular direction, forming this magnetization pattern. Every pattern in the CMG structure is oriented parallel to the opposing flux line [14].

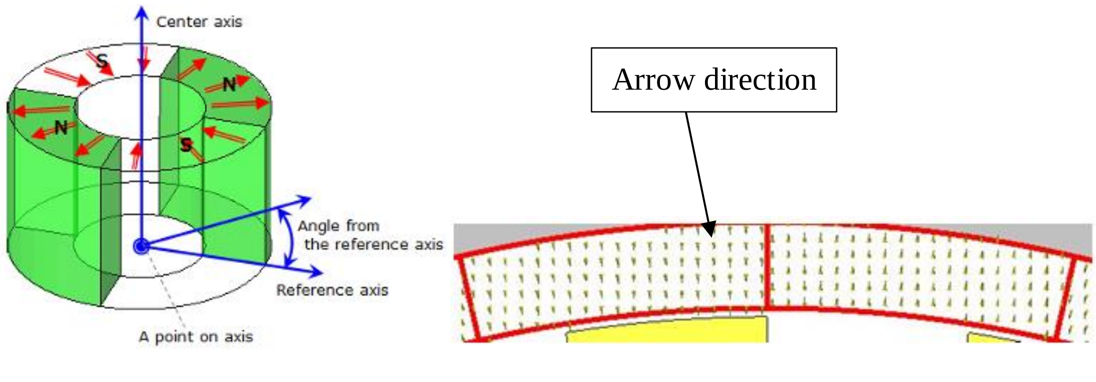

Figure 2.8: Parallel Pattern Radial Direction (PRD) [14]

2.2.5 Comparison of Magnetic Gears

Magnetic gears are an appealing option in a variety of applications because they have significant benefits over conventional mechanical gears. The following are some contrasts between each magnetic gear [3]:

Table 2.1: Comparison of each Magnetic Gears

Specification	**Concentric Magnetic Gear** [7][3]	**Harmonic Magnetic Gear** [2][3]	**Planetary Magnetic Gear** [5][3][6]
Structure	Coaxial arrangement of magnets	Uses flexible magnetic coupling	Consist of magnetic planets, sun and ring
Torque Density	Moderate to high	High	Very high
Torque Ripple	Low to moderate	Very low	Low
Efficiency	High (typically>95%)	High (typically>90%)	High (typically>95%)
Speed Ratio	Moderate (typically 2:1 to 10:1)	High (up to 100:1 or more)	Variable (depends on configuration)
Size and Weight	Compact but larger than harmonic gears	Very compact	Can be bulky depending on the application
Complexity	Simple to assemble	High Complexity	Low complexity
Vibration and Noise	Very low	Very low	Low
Manufacturing Cost	Moderate	High due to complexity	Moderate to high
Applications	General machinery, robotics and automotive	Precision robotics, aerospace	Heavy machinery, wind turbines

2.3 Parameters of Magnetic Gears

Different magnetic gears were simulated in this work using arbitrarily varied parameters. This was carried out in order to examine the gearbox torque characteristic in relation to the total PM volume. In order to guarantee uniformity in the characteristics of the simulated magnetic gears, a few parameters are set, as indicated in Table 2.2. A high-speed rotor running at 1000 rpm may be reduced to a low-speed rotor running at 200 rpm thanks to a fixed 5:1 gear ratio [15]. For applications requiring less torque enhancement, this low gear ratio is appropriate. Nonetheless, a double-stage gearing ratio of 25:1 is regarded as excessive. The majority of gear applications such as those using induction motors and DC motors depend on the speed of the prime mover, which is why 1000 rpm is chosen as the input speed [15][16].

Table 2.2: Value of fixed parameter of the Magnetic Gears [15]

Design Parameter	**Value**
Gear Ratio, G_r	5:1
Speed of high-speed rotor, n_{hs}	1000rpm
Speed of low-speed rotor, n_{ls}	200rpm
Number of pole-pairs at HS rotor, p_{hs}	2
Number of pole-pairs at LS rotor, p_{ls}	10
Number of pole pieces, N_{pp}	12
Length of air gap, g	0.5mm

There are two pole pairs at a high-speed rotor, requiring four PMs, and ten pole pairs at a low-speed rotor, requiring twenty PMs. Equation 10 indicates that the total number of pole pairs at both high-speed and low-speed rotors equals 12, which is the number of pole pieces. Because smaller air gaps boost permeance and lower flux resistance, the magnetic gears are made with 0.5 mm air gaps between the rotors and the pole pieces. As it has been demonstrated that air gaps smaller than 0.5 mm can also be accomplished when building an electric machine, there is no problem with the assembly process [15].

$$N_{pp} = P_{high\ speed} + P_{low\ speed} = \frac{N_{high\ speed} + N_{low\ speed}}{2} \qquad (10)$$

UNIVERSITI TEKNIKAL MALAYSIA MELAKA

The size of the magnetic gears' construction, as seen in Figure 2-9, is a variable parameter, whereas Table 2-2 displays the fixed values. The parameters that have undergone changes include the MG outer radius (r_{out}) and inner radius(r_{in}), outer yoke thickness(t_{out}), low speed rotor PM thickness(t_{m2}), pole piece thickness(t_p), high speed rotor PM thickness(t_{m1}), and inner yoke thickness(t_{in}) [15].

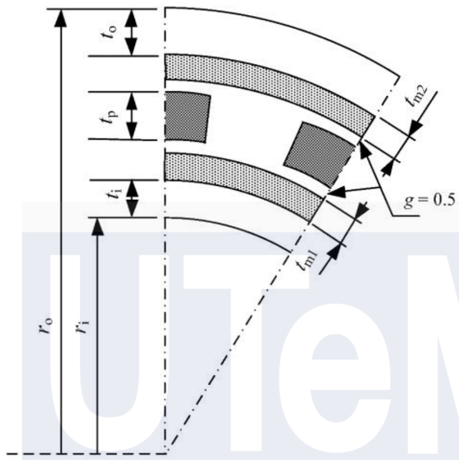

Figure 2.9: Parameters of surface type of PM Concentric Magnetic Gears (CMG)[15]

2.4 Torque density of Magnetic Gears

UNIVERSITI TEKNIKAL MALAYSIA MELAKA

A few magnetic gear models were used in the testing process to demonstrate the significance of the Maximum Transmission Torque Line for surface type magnetic gear design [15]. To confirm that the suggested method is appropriate, five models of magnetic gears were arbitrarily created under various situations while taking the Maximum Transmission Torque Line into account. Given that the Maximum Transmission Torque Line is constrained by the fixed requirements [15], these conditions were adhered to throughout the model's construction. Every model need, as indicated in Table 2-3, is comprised of a necessary magnetic gear radius and a targeted gearbox torque that randomly reflect different types of applications. Models 1 and 4 sought 100 Nm and 85 Nm of gearbox torque for the MG, respectively, and required 160 mm of diameter. In contrast, Model 2 needed 140 Nm of torque and a magnetic gear with a 240 mm diameter. Model 3 sought a magnetic gear with a diameter of 390 mm and a gearbox torque of 200 Nm. Last but not least, Model 5 sought a gearbox torque of 60 Nm and needed 120 mm in diameter. The thickness of the permanent magnet and other parameters are obtained by substituting the required radius of the magnetic gear, the total volume of PMs, and the length of the magnetic gear into the equations [17]. The maximum gearbox torque line yields the total volume of PMs from the specific targeted torque. In order to determine the outcome of the simulated gearbox torque, all of the models were created using the parameters that were collected and are displayed in Table 2.3. The Finite Element Method was then used for analysis. The percentage of inaccuracy is obtained to correlate with the applicability of the Maximum Transmission Torque Line for building coaxial magnetic gear by comparing the simulated and intended transmission torque of the models [15].

Table 2.3: Conditions and parameters for design verification of Magnetic Gears[15]

Model	Design requirement		Estimated Parameter					
	Transmission Torque, T_{ls} (Nm)	**Outer Radius, R_o (mm)**	V_{pm} **(cm^3)**	ℓ **(mm)**	t_{pm} **(mm)**	t_p **(mm)**	t_o **(mm)**	t_i **(mm)**
1	100	80	179	70	3.3	8.3	13.2	16.5
2	140	120	250	50	4.5	11.3	18.0	22.5
3	200	195	357	30	6.0	15.0	24.0	30.0
4	85	120	152	30	4.5	11.3	18.0	22.5
5	60	60	107	70	3.0	7.5	12.0	15.0

2.5 Summary

Choosing a Concentric Magnetic Gear can be beneficial for a number of reasons, depending on the demands of the particular application. This is because Concentric Magnetic Gears offer an excellent trade-off between torque output and size. They aren't overly big, but they can produce a lot of torque. For many applications, these gears' smooth and steady functioning is ensured by their relatively minimal torque ripple [10]. Concentric magnetic gears usually have high efficiencies (typically >95%), meaning that there is little energy lost when power is transferred. For situations where energy saving is critical, this efficiency is vital. Concentric magnetic gears are less complicated to make and maintain than planetary and harmonic magnetic gears because of their simpler design. Higher dependability and simplicity of maintenance are frequently associated with simple designs, which can be crucial for applications that call for trouble-free, long-term operation. Because of their versatility, concentrated magnetic gears find application in a wide range of industries, including as robotics, general machinery, and the automobile industry. They are appropriate for a wide range of mechanical systems due to their capacity to manage varying torque and speed requirements. Concentric magnetic gears are typically less expensive than harmonic and planetary magnetic gears, even if they aren't as cheap as certain traditional mechanical gears. This is especially true when taking into account the trade-off between performance and complexity. The necessity for a dependable, cost-effective, and reasonably priced option that provides a good combination of torque density and smooth operation frequently motivates the selection of a Concentric Magnetic Gear [10]. They are particularly well suited for situations where these characteristics take precedence over the exceptionally high torque capacity of planetary gears or the incredibly high accuracy or compact size provided by harmonic gearClick or tap here to enter text..

UNIVERSITI TEKNIKAL MALAYSIA MELAKA

CHAPTER 3

METHODOLOGY

3.1 Introduction

In this chapter will go into additional detail about the project's journey from inception to goal achievement. It includes tactics that will be applied to every aspect of the request in order to achieve the project's objectives.

3.2 Project Structure

In many industrial applications, Concentric Magnetic Gears without winding have drawn a lot of attention as an alternative to conventional mechanical gears. These gears enable non-contact power transmission by using magnetic fields to transfer torque between the driven and driving shafts without requiring physical contact.

The goal of the project is to investigate the design and optimisation of winding-free concentric magnetic gears, with an emphasis on gears with fewer pole pairs. Potential benefits of a decreased pole pair number include a higher torque density, less cogging effects, increased efficiency at low speeds, streamlined production procedures, and simpler alignment during assembly.

The research aims to analyse and model the behavior of the concentric magnetic gear by utilizing software tools such as JMAG Designer. This will provide a comprehensive knowledge of the torque gearbox capabilities, overall performance characteristics, and magnetic interactions. Based on the analytical findings, design iterations and optimisations will be carried out to improve the gear's performance and meet the intended goals.

UNIVERSITI TEKNIKAL MALAYSIA MELAKA

In addition, the study will compare gears with greater pole pair numbers to concentric magnetic gears with lesser numbers. The benefits and drawbacks of various gear designs will be evaluated with the use of this comparative study, which will take into account variables including torque density, cogging effects, efficiency at various speeds, manufacturing complexity, and alignment requirements. The objective is to ascertain the best design for certain uses and offer information on the benefits of fewer pole pair numbers in concentric magnetic gears.

The project's overall goal is to advance knowledge of concentric magnetic gear technology without winding, with a focus on gears that have fewer pole pairs. This will open the door to more creative and effective torque transfer solutions across a range of industries.

3.3 Project Flowchart

This flowchart is designed to offer a comprehensive visual representation of the project's workflow, detailing each phase from initiation to completion. By mapping out the steps and processes, it aim to facilitate a clear understanding of the project's structure, ensuring aligned with the project's objectives and timelines.

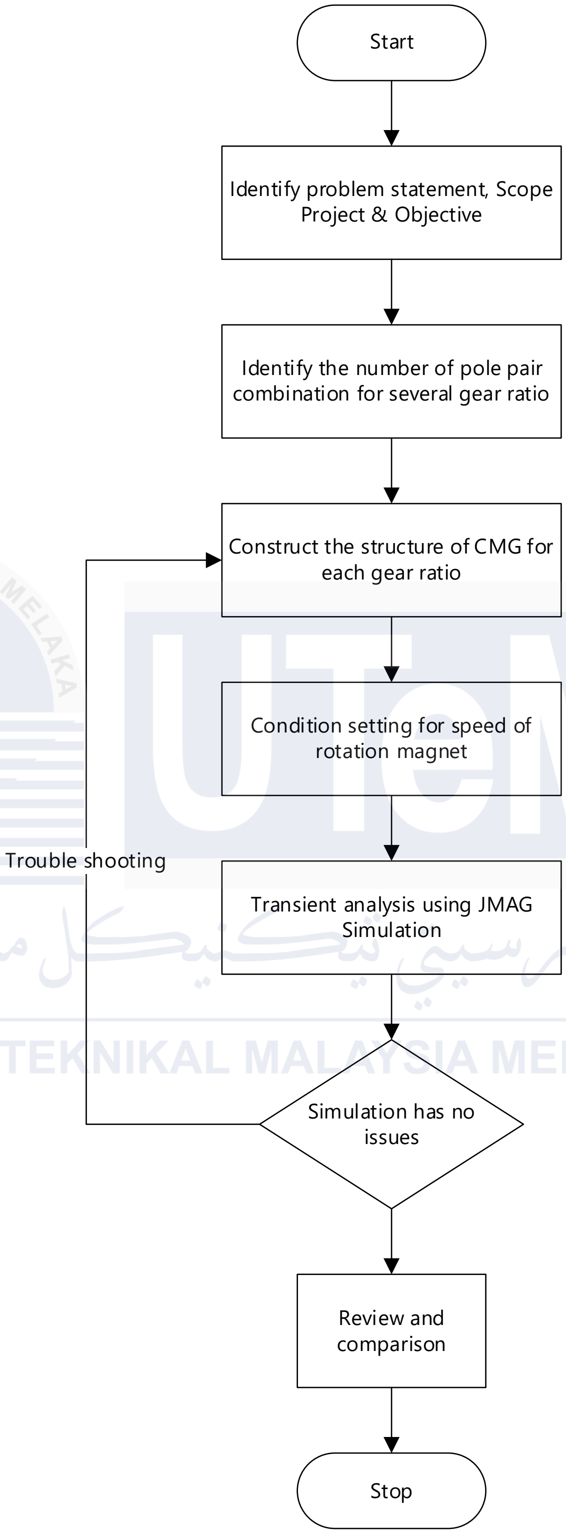

Figure 3.1: Project Flowchart

UNIVERSITI TEKNIKAL MALAYSIA MELAKA

3.4 Working Principles

This process of creating and deploying a concentric magnetic gear follows an organised approach that starts with comprehending the application's needs, which include torque, speed, and space limitations. Subsequently, appropriate materials for the structural and magnetic components are chosen, and certain gear characteristics are established. Using JMAG-Designer software, the gear's layout is created. Finite Element Method (FEM) is then used to analyse the magnetics and simulate performance [18][19]. Test findings are used to improve and optimise the design. This thorough approach guarantees a concentric magnetic gear system that is well-designed, highly dependable, and performs well [19].

3.5 Theoretical of Concentric Magnetic Gears

When the pole piece functions as a rotor, an equation is constructed and solved in the project's first section. comprehension the torque behaviour under certain circumstances requires a comprehension of this mathematical concept. According to Equation 11, the total number of pole pieces in the concentric magnetic gear is equal to the sum of the pole pairs on the outer and inner rotors [9] [20].

$$P_{in} + P_{Out} = Ns \tag{11}$$

By dividing the number of teeth on the output rotor by the number of teeth on the input rotor, one may compute the gear ratio in Equation 12. The relationship between the two rotors' rotational speeds in a gear system may be measured using this ratio [11][12].

$$G_r = \frac{P_o}{P_i} \tag{12}$$

Equation 13 uses the gear ratio (Gr) and the speed of one of the rotors to get the speed (rotations per minute, rpm) [11].

$$N_{out} = \frac{N_{in}}{G_r} \tag{13}$$

The formula to compute the time interval (Δt) depending on the speed in revolutions per minute (rpm) is represented by Equation 14 [5].

$$\Delta t = \frac{1}{speed} x\ 60 \tag{14}$$

Utilising these numbers from Equation 15, compute the torque ripple as a percentage using the formula. Stable performance is suggested if the outcome is near the gear ratio [21][22].

$$Torque\ ripple = \frac{Torque_{max} - Torque_{min}}{Torque_{avg}} x\ 100 \tag{15}$$

The ratio of the outer rotor average to the inner rotor average may be found using equation 16. This outcome is rather near to the intended gear ratio. It shows that the predicted gear ratio and the observed torque ripple data are well aligned [12].

$$G_r = \frac{N_{out}}{N_{in}} \tag{16}$$

3.6 Final element JMAG-Designer configuration

The JMAG Simulation Setup, a crucial part of the approach intended to investigate the performance characteristics of Concentric Magnetic Gears (CMGs), is described in this section. Using JMAG Designer, an advanced electromagnetic simulation programme, provides a thorough framework for investigating the dynamic behaviour of the CMG system. To create a virtual environment for in-depth investigation, the simulation setup entails converting theoretical formulations and derived equations into a 2D Finite Element Method (FEM) simulation [18][23]. The particular parameters, settings, and circumstances used in JMAG Designer (version 18.1) to run simulations at various rotational speeds are described in this section. The simulations validate steady-state waveform conditions by progressively increasing the rotational speed of the inner rotor, which starts at 400 rpm. The aim is to investigate how the CMG reacts to various operating situations and comprehend its effectiveness and performance patterns [20].

3.6.1 Number of pole pair and gear ratio

Table 3.2 use simulations to determine eddy current loss and iron loss, analyse torque ripple, compute gear efficiency at various rotational speeds, and evaluate different pole pair combinations to achieve different gear ratios [24].

Table 3.1: Comparison of number pole pair and gear ratio

Design	Inner pole pair	Outer pole pair	Ferromagnetic pole	Gear ratio
Combination 1	4	12	16	3
combination 2	4	14	18	3.5
Combination 3	4	18	22	4.5
Combination 4	4	22	26	5.5
Combination 5	4	24	28	6
Combination 6	2	6	8	3
Combination 7	2	7	9	3.5
Combination 8	2	9	11	4.5
Combination 9	2	11	13	5.5
Combination 10	2	12	14	6
Combination 11	4	12	16	3

UNIVERSITI TEKNIKAL MALAYSIA MELAKA

Combination 12	4	14	18	3.5
Combination 13	4	18	22	4.5
Combination 14	4	22	24	5.5
Combination 15	4	24	28	6
Combination 16	2	6	8	3
Combination 17	2	7	9	3.5
Combination 18	2	9	11	4.5
Combination 19	2	11	13	5.5
Combination 20	2	12	14	6

3.6.2 Comparison of speed in Rpm

The various rotational speed combinations for the Concentric Magnetic Gear (CMG) mechanism are shown in this Table 3.1. This parameters allow for changes in the inner and outer rotor speeds, which allows for a thorough investigation of the CMG's performance in various operational scenarios.

Table 3.2: Speed comparison on combination 1-5

Combination	**1**		**2**		**3**		**4**		**5**	
Rotor speed (rpm)	Inner	Outer	Inner	Outer	Inner	Outer	Inner	Outer	Inner	Outer
	1200	400	1400	400	1800	400	2200	400	2400	400

UNIVERSITI TEKNIKAL MALAYSIA MELAKA

Table 3.3: Speed comparison on combination 6-10

Combination	**6**		**7**		**8**		**9**		**10**	
Rotor speed (rpm)	Inner	Outer	Inner	Outer	Inner	Outer	Inner	Outer	Inner	Outer
	600	200	700	400	900	200	1100	200	1200	200

Table 3.4: Speed comparison on combination 11-15

Combination	**11**		**12**		**13**		**14**		**15**	
Rotor speed (rpm)	Inner	Outer	Inner	Outer	Inner	Outer	Inner	Outer	Inner	Outer
	1200	400	1400	400	1800	400	2200	400	2400	400

Table 3.5: Speed comparison on combination 16-20

Combination	**16**		**17**		**18**		**19**		**20**	
Rotor speed (rpm)	Inner	Outer	Inner	Outer	Inner	Outer	Inner	Outer	Inner	Outer
	600	200	700	200	900	200	1100	200	1200	200

UNIVERSITI TEKNIKAL MALAYSIA MELAKA

3.6.3 Material used for Concentric Magnetic Gear

The choice of material shown in figure 3.2 and figure 3.3 is an important consideration that greatly affects a system's performance and outcomes, particularly in situations where electrical conductivity and magnetic fields are involved, as in the case of Concentric Magnetic Gears (CMGs). Here are some important things to think about when deciding what materials to use and how they affect CMG performance [24].

3.6.3.1 35H210 NIPPON STEEL

Because of its many benefits, steel grade 35H210 is widely prized in a variety of industrial and technological fields. It is especially well-suited for electronic and electrical components including motors, inductors, and transformers because of its remarkable magnetic qualities, which include low core loss and high permeability. By lowering losses and guaranteeing efficient magnetic performance, these characteristics improve energy efficiency. Furthermore, 35H210 has strong tensile strength and ductility, which increase its dependability and durability under mechanical stresses and allow for extended usefulness. It is appropriate for applications needing thermal stability because of its capacity to retain mechanical and magnetic properties in the face of temperature fluctuations.

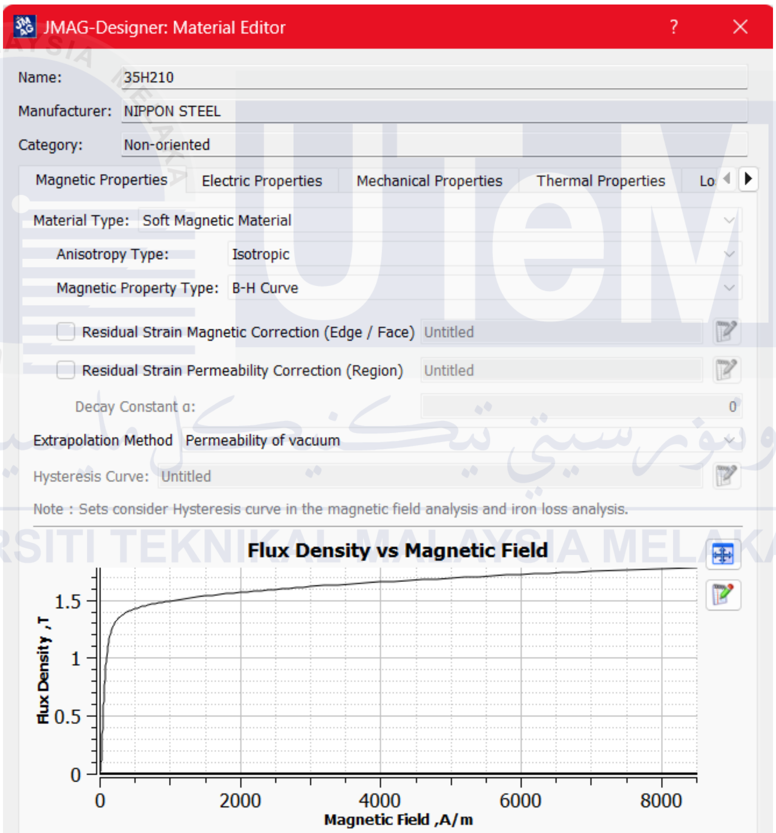

Figure 3.2: 35H210 Material properties

3.6.3.2 NdFeB_Br=1.2(T) JSOL

Because of their high magnetic properties, Neodymium Iron Boron (NdFeB) magnets with a residual magnetic flux density (B_r) of 1.2 Tesla (T) have several benefits. Their strong magnetic field enables the production of smaller, lighter magnets without sacrificing their functionality in comparison to bigger ones built of different materials[25].

UNIVERSITI TEKNIKAL MALAYSIA MELAKA

Because of its high magnetic strength, a variety of devices, including electric motors, generators, and magnetic separators, operate more efficiently and use less energy. High flux densities in motor applications lead to higher torque and power densities, which improve the efficiency and potency of motors[25].

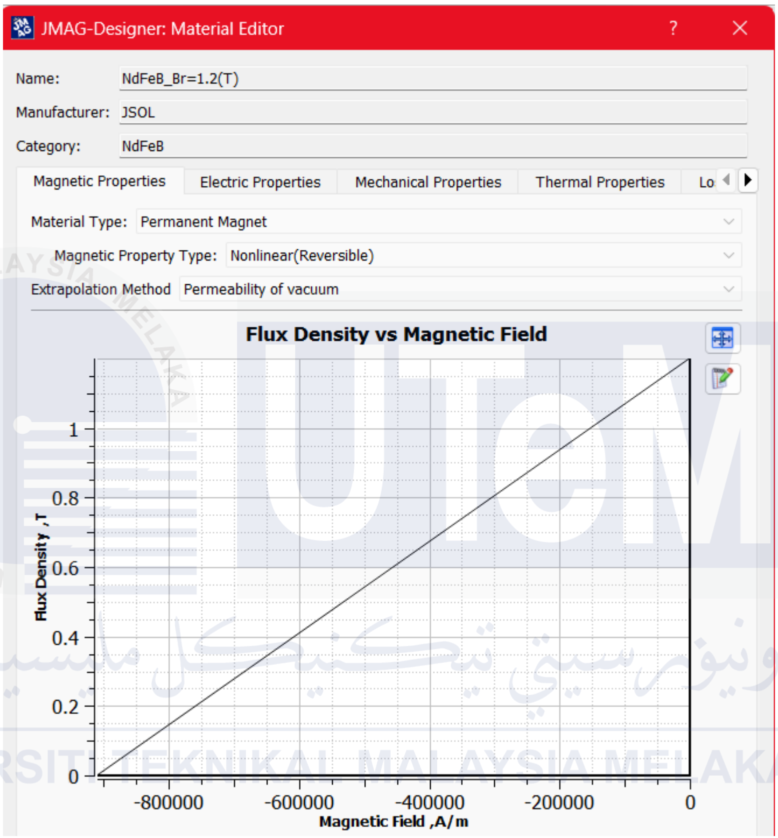

Figure 3.3: NdFeB_Br=1.2(T) JSOL Material properties

3.6.4 Material selection for each part in Concentric Magnetic Gear

Table 3.3 presents comprehensive details on the materials utilised for every system component, including their corresponding resistivity values. Particularly in applications involving magnetic fields and electrical conductivity, the resistivity is an essential metric for comprehending the electrical properties of the materials.

UNIVERSITI TEKNIKAL MALAYSIA MELAKA

Table 3.6: Material for each part in Concentric Magnetic Gear

Part	Material	Resistivity
Inner rotor backiron	35H210	5.9e-7 ohm m
Inner rotor magnetic poles	NdFeB_Br=1.2(T)	1.4e-6 ohm m
Ferromagnetic poles	35H210	5.9e-7 ohm m
Outer rotor magnetic poles	NdFeB_Br=1.2(T)	1.4e-6 ohm m
Outer rotor backiron	35H210	5.9e-7 ohm m

3.6.5 Setup of time interval

The Concentric Magnetic Gear (CMG) system's time interval settings are described in this Table 3.4. This parameter is essential to comprehending the system's dynamic behaviour.

UNIVERSITI TEKNIKAL MALAYSIA MELAKA

Table 3.7: Time interval for each design

Design	Inner rotor	Outer rotor	Time Interval (s)
1	1200 rpm	400 rpm	0.05
2	1400 rpm	400 rpm	0.043
3	1800 rpm	400 rpm	0.033
4	2200 rpm	400 rpm	0.027
5	2400 rpm	400 rpm	0.025
6	600 rpm	200 rpm	0.1
7	700 rpm	200 rpm	0.086
8	900 rpm	200 rpm	0.067
9	1100 rpm	200 rpm	0.055
10	1200 rpm	200 rpm	0.05
11	1200 rpm	400 rpm	0.05

12	1400 rpm	400 rpm	0.043
13	1800 rpm	400 rpm	0.033
14	2200 rpm	400 rpm	0.027
15	2400 rpm	400 rpm	0.025
16	600 rpm	200 rpm	0.1
17	700 rpm	200 rpm	0.085
18	900 rpm	200 rpm	0.067
19	1100 rpm	200 rpm	0.055
20	1200 rpm	200 rpm	0.05

اونيورسيتي تيكنيكل مليسيا ملاك
UNIVERSITI TEKNIKAL MALAYSIA MELAKA

3.7 Geometric JMAG-Designer

JMAG-Designer is a comprehensive simulation software used for the analysis and design of electromagnetic components and systems. The essential elements and variables that specify the electromagnetic configuration of the CMG are depicted in this diagram. This picture, which was created using specialised design software called JMAG Designer, captures the details of the CMG construction, such as the placement of the magnets and pole components as well as the many measurements that go into determining the gear ratio. For CMG systems with an appropriate gear ratio, the design provides a visual aid for comprehending the geometric and electromagnetic elements that are essential to attaining the intended performance.

The process of creating a magnetic gear using JMAG-Designer software, which is a crucial stage in the creation of Concentric Magnetic Gear, is depicted in the diagram below. Using JMAG-Designer, a complete model of the electromagnetic components of the CMG, including the outer rotor backiron, outer rotor magnetic poles, and ferromagnetic poles, must be created at this first design stage. Through the use of the software's sophisticated modelling features, it is possible to precisely forecast the interactions between the electromagnetic fields inside the Magnetic Gear, measure the impacts of heat, and analyse the structural integrity.

This first model allows for the early detection and mitigation of any problems in the design process by providing a blueprint for subsequent optimisation and refining. JMAG-Designer software facilitates the development of a Concentric Magnetic Gear that is both extremely efficient and dependable, guaranteeing excellent performance in practical applications through iterative simulations and modifications.

UNIVERSITI TEKNIKAL MALAYSIA MELAKA

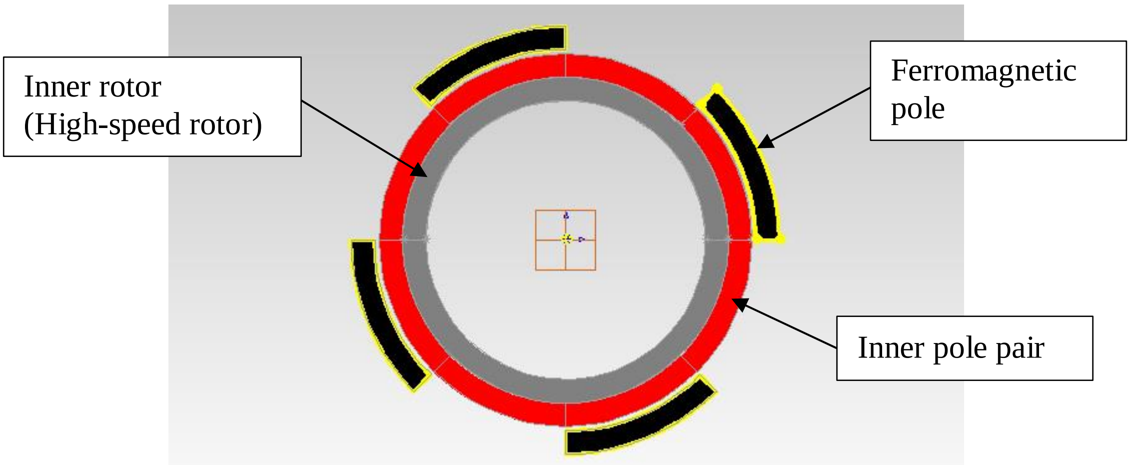

Figure 3.4: Magnetic Gear geometry design

The Concentric Magnetic Gear (CMG) magnet design is finished after the first design stage, as the diagram below illustrates. At this point, the particular specifications for the magnetic components are finalised, and it is made sure that the design satisfies all performance and efficiency requirements. It carefully simulates the magnetic fields and their interactions inside the CMG using the JMAG-Designer software in order to maximise the magnetic circuit, reduce losses, and guarantee reliable performance across a range of operating circumstances.

UNIVERSITI TEKNIKAL MALAYSIA MELAKA

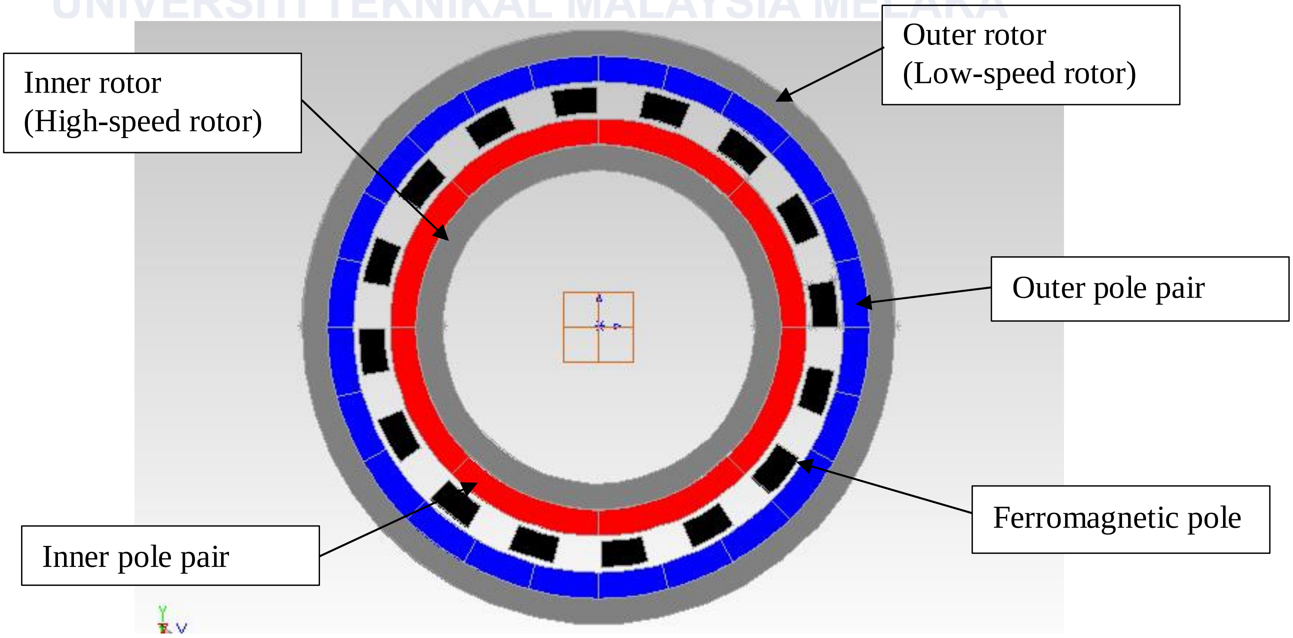

Figure 3.5: Completed design of Concentric Magnetic Gear

A comprehensive summary of the Concentric Magnetic Gear (CMG) option that is especially suited is given in Table 3.8, Table 3.9, Table 3.10, Table 3.11 and Table 3.12. These specified criteria include numbers of pole pairs, radius, rotating speeds, air gap widths, and other variables that are essential to reaching the desired gear ratio.

Table 3.8: Properties of CMG part

Types of part	Value
Magnetic Gear radius	90
Inner pole radius	35.00
Outer pole radius	47.00
Stack length	30mm
Inner magnet width	5mm
Outer magnet width	5mm
Inner pole angle (^{o})	45.00
Ferromagnetic radius	41.00
Air gap for combination 1-10	1mm
Air gap for combination 11-20	2mm

UNIVERSITI TEKNIKAL MALAYSIA MELAKA

Table 3.9: Parameter of combination 1-5

Parts	Design 1	Design 2	Design 3	Design 4	Design 5
Gear Ratio	3	3.5	4.5	5.5	6
Inner pole pair	4	4	4	4	4
Outer pole pair	12	14	18	22	24
Ferromagnetic pole	16	18	22	26	28
Outer pole angle (^{o})	15.00	12.86	7.50	8.18	7.50
Ferromagnetic angle (^{o})	11.25	10.00	8.18	6.92	6.43

Table 3.10: Parameter of combination 6-10

Parts	Design 6	Design 7	Design 8	Design 9	Design 10
Gear Ratio	3	3.5	4.5	5.5	6
Inner pole pair	2	2	2	2	2
Outer pole pair	6	7	9	11	12
Ferromagnetic pole	8	9	11	13	14
Outer pole angle (^{0})	30.00	25.71	20.00	16.36	15.00
Ferromagnetic angle (^{0})	22.50	20.00	16.36	13.85	12.85

Table 3.11: Parameter of combination 11-15

Parts	Design 11	Design 12	Design 13	Design 14	Design 15
Gear Ratio	3	3.5	4.5	5.5	6
Inner pole pair	4	4	4	4	4
Outer pole pair	12	14	18	22	24
Ferromagnetic pole	16	18	22	26	28
Outer pole angle (^{0})	15.00	12.85	10.00	8.18	7.50
Ferromagnetic angle (^{0})	11.25	10.00	8.18	6.92	6.42

Table 3.12: Parameter of combination 16-20

Parts	Design 16	Design 17	Design 18	Design 19	Design 20
Gear Ratio	3	3.5	4.5	5.5	6
Inner pole pair	2	2	2	2	2
Outer pole pair	6	7	9	11	12
Ferromagnetic pole	8	9	11	13	14
Outer pole angle (^{0})	30.00	25.71	20.00	16.36	15
Ferromagnetic angle (^{0})	22.50	20	16.36	13.85	12.85

اونيۏرسيتي تيكنيكل مليسيا ملاك
UNIVERSITI TEKNIKAL MALAYSIA MELAKA

3.8 Pattern Selection for Concentric Magnetic Gear

Finding the right pattern has a big impact on the magnetic response, thus choosing the right one is essential to getting the best outcomes. CMG has used a Radial Anisotropic Pattern to address this. This particular design improves the alignment of magnetic domains, which raises the magnetic system's overall performance and efficiency. CMG makes sure that the magnetic characteristics are optimized by carefully selecting this pattern, which produces better results in their applications. Figure 3.6 shows the pattern that has been inserted into each inner pole pair and outer pole pair magnet.

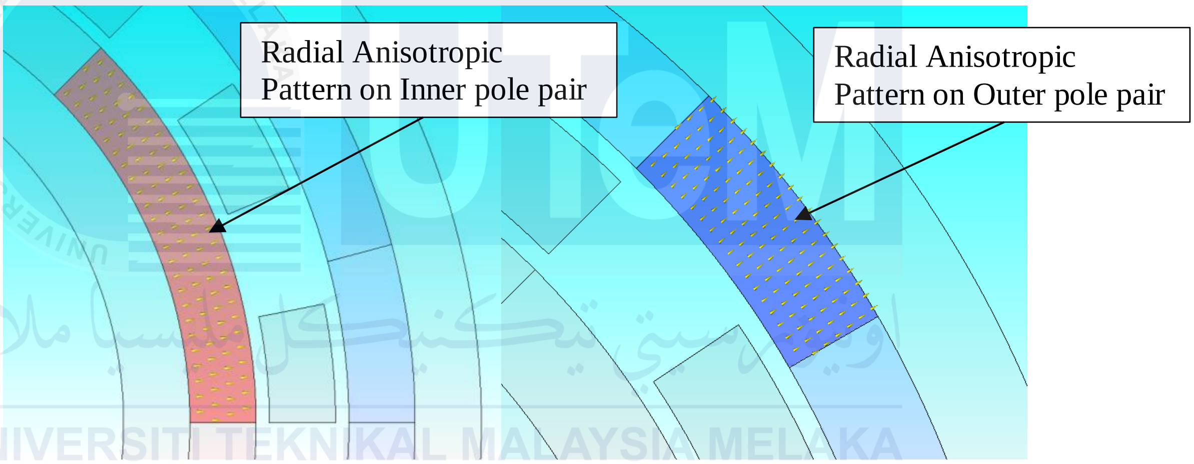

Figure 3.6: Radial Anisotropic Pattern on Inner and Outer Pole Pair Magnet

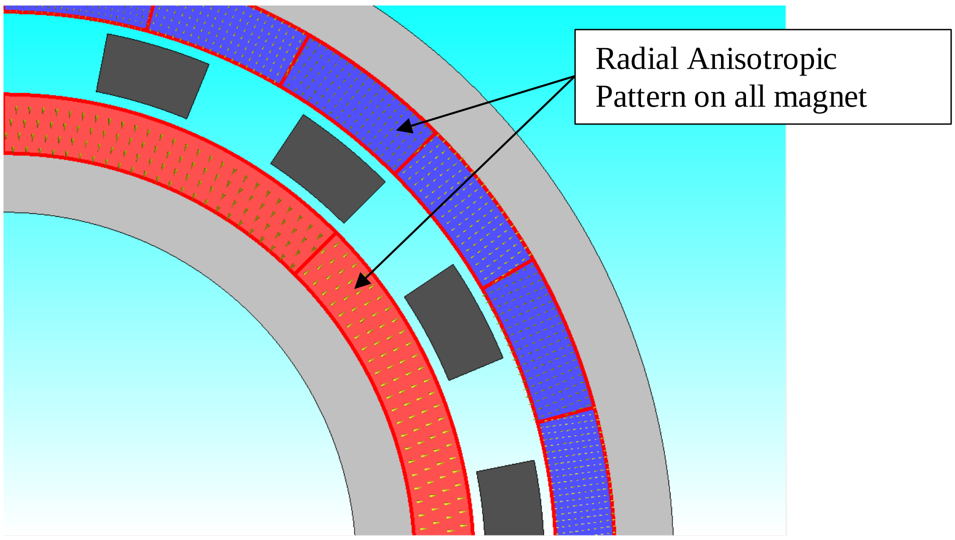

Figure 3.7: Completed pattern on all magnet

3.9 Software setting

The setting of magnetic gear involves configuring the magnetic components to achieve desired performance and functionality. This process includes determining the step control, full model conversion and slide division. All these settings apply to all design of Concentric Magnetic Gear.

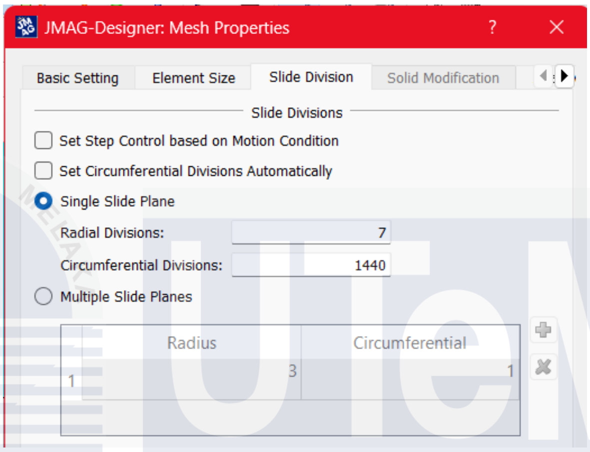

Figure 3.8: Slide Division setting

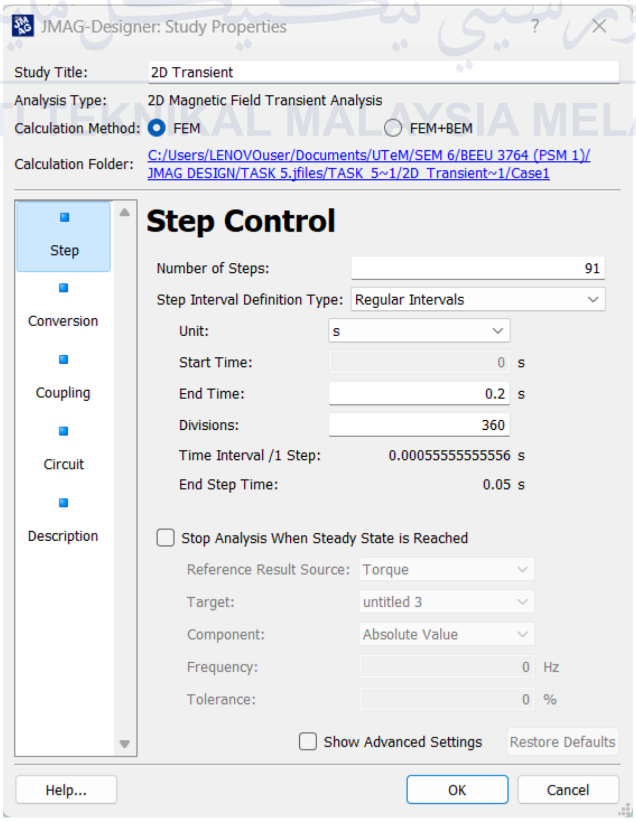

Figure 3.9: Step control setting

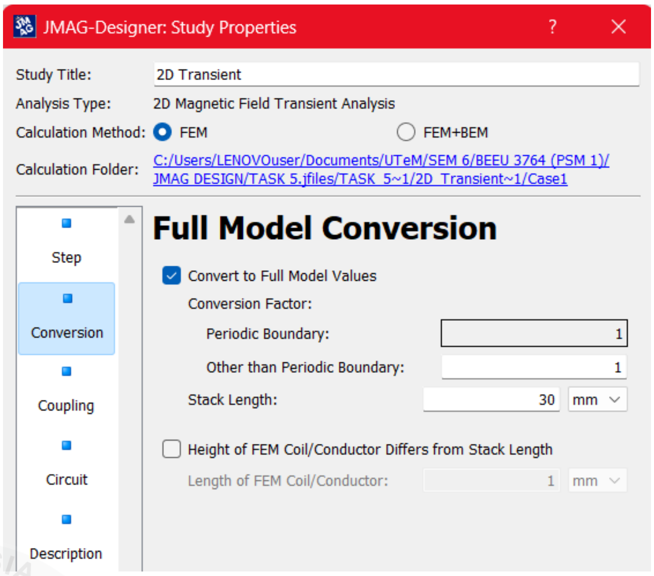

Figure 3.10: Full Model Conversion setting

3.10 Conclusion

In order to study the torque behaviour of Concentric Magnetic Gears (CMGs) for electric vehicle applications, this research project uses a thorough four-part methodology that combines mathematical derivation, electromagnetic simulation using JMAG Designer, pole pair combination evaluation, and material selection. The optimisation of CMG design for electric vehicle applications is facilitated by the obtained equations, simulation results, and material selections. The results provide a useful starting point for next experimental investigations and direct the creation of effective and superior CMGs for real-world applications in electric cars.

UNIVERSITI TEKNIKAL MALAYSIA MELAKA

CHAPTER 4

RESULTS AND DISCUSSIONS

4.1 Introduction

The results of the project simulations used to assess Concentric Magnetic Gears (CMG) for use in electric vehicle applications are presented and discussed in this chapter. It seeks to highlight important discoveries and their ramifications through a succinct presentation of the findings and a thorough discussion. This chapter looks into torque characteristics and the effects of different pole pair combinations in an effort to offer insights that aid in the comprehension and improvement of CMG performance.

Because of their distinct benefits over conventional mechanical gears, CMG are being explored more and more for use in electric vehicle (EV) applications. Because of its many benefits, including its high efficiency resulting from the lack of direct mechanical contact and its ability to reduce frictional losses, CMG was chosen as the best option based on the findings of the previous study. As a result, energy efficiency is increased, and EV range may be increased. Magnetic gears are less prone to wear and tear since there is no physical contact between the moving parts. When compared to conventional gears, this means less maintenance needs and a longer lifespan. Additionally, CMG offers built-in safety against torque overload by sliding under extreme torque, hence avoiding harm to the drivetrain's constituent parts. This feature improves the EV's robustness and security. Through establishing a link between theoretical predictions and observable results, this discussion hopes to stimulate more study and developments in CMG technology.

4.2 Results and Analysis

The graph serves as a valuable tool for assessing the impact of various pole pair combinations and rotational speeds on torque fluctuations. Through these graphical representations, trends, patterns, and correlations within the ripple vs torque data become apparent, contributing to a deeper insight into the behavior of the CMG system. The interpretation of these ripple vs torque graphs plays a pivotal role in drawing conclusions regarding the optimization and efficiency of the CMG for electric vehicle applications. In the analysis of graph for the CMG system with different configurations in Figure 4.1 , 4.2 ,4.3, and 4.4), the graphical representation reveals distinct patterns and variations in ripple and torque behavior.

4.3 Relationship between Ripple vs Torque

The data presented in Figure 4.1, Figure 4.2, Figure 4.3, Figure 4.4 and Figure 4.5 illustrates the relationship between torque ripple and torque across twenty different combinations, each characterized by varying gear ratios of 3, 3.5, 4.5, 5.5, and 6. This analysis is crucial for understanding how torque ripple behaves under different mechanical configurations.

4.3.1 Graph Ripple vs Torque for Combination 1-5

Combination 1 has the lowest inner ripple percentage at 111.65%, much higher than other combinations, which shows great instability. A low outer ripple percentage of 9.53% indicates that, similar to inner fluctuations, although there are many inner fluctuations, the outer performance is relatively stable. The average inner torque is 28.60 Nm and the outer is 18,41 Nm, both quite high. This combination suggests that controlling its internal dynamics may have a design flaw and finding blade alignment or balancing the flow would be the mitigation strategy.

Combination 2, the inner ripple is significantly reduced to only 2.74%, showing significant stability improvements. Then the outer ripple percentage also shrinks to just 0.08%, which is the most stable of all combinations. According to torque data in newton-meters (Nm), Values of average inner torque and average outer torque are 29.31 Nm and 8.37 Nm respectively. This result indicates that the design adjustment has minimized ripples dramatically at the expense of inner torque performance, indicating an optimum condition for outer ripple minimization.

In comparison to Combination 2, Combination 3 exhibits a moderate increase in instability with an inner ripple rebound to 40.13%. A change in performance focus is reflected in the outer ripple, which marginally increases but stays low at 6.14%. While the average outer torque increases to 10.22 Nm, the average inner torque slightly decreases to 27.82 Nm, indicating a compromise design that attempts to maintain moderate torque levels while balancing inner and outer stability.

Combination 4 shows an Inner ripple decreasing to 1.82%, once more highlighting impressive inner stability, similar to Combination 2. The external ripple percentage stays low at 0.08%, indicating consistency from outside. Nevertheless, the average inner torque decreases further to 28.21 Nm, while the outer torque slightly reduces to 5.12 Nm. This blend might be seen as an enhanced iteration of Combination 2, where ripple percentages are reduced with marginally affected torque outputs.

In Combination 5, the inner ripple percentage increases once more to 48.33%, indicating instability akin to Combination 3. The external ripple, however, stays stable at 4.43%, signaling a better equilibrium compared to Combination 1 but not as advantageous as Combinations 2 and 4. The average inner torque reduces to 26.85 Nm, the smallest of all combinations, and the outer torque drops to 4.43 Nm as well. This setup could be useful in scenarios where slight outer instability is tolerable, although inner instability remains a disadvantage.

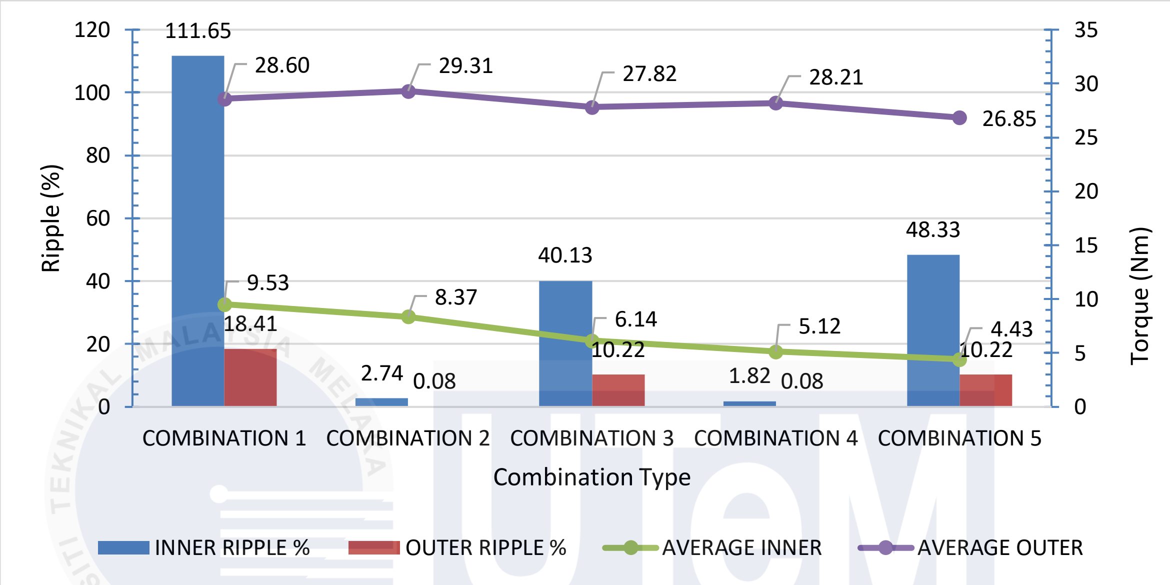

Figure 4.1: Graph Ripple vs Torque for Combination 1-5

4.3.2 Graph Ripple vs Torque for Combination 6-10

Combination 6 exhibits a remarkably high inner ripple percentage of 209.61%, the highest of all combinations, suggesting considerable instability within the system. The outer ripple percentage, recorded at 50.24%, is notably high when compared to other combinations. The typical inner torque measures 14.80 Nm, while the outer torque is 7.30 Nm, with both values being moderate. This pairing shows inadequate design efficiency and stability, featuring excessive ripples that indicate potential problems such as turbulence or imbalance in the system's dynamics.

The inner ripple percentage significantly drops to 4.93%, indicating a noteworthy enhancement in stability relative to Combination 6. The outer ripple percentage also decreases notably to 0.51%, indicating strong outer stability. The mean inner torque is 16.88 Nm, while the outer torque measures 4.82 Nm, signifying a balanced setup that emphasizes stability and sustains acceptable torque performance. This combination is very effective for uses that demand both minimal ripple and steady torque output.

In this combination 8, the inner ripple rises slightly to 6.62%, yet it stays within acceptable limits. The outer ripple rate decreases to 0.38%, signifying ongoing outer stability. The typical inner torque marginally drops to 19.59 Nm, whereas the outer torque reduces to 4.35 Nm. This configuration illustrates a compromise design that preserves ripple stability while optimizing torque output to a moderate extent. It is perfect for systems that prioritize minimal external variations.

The inner ripple decreases even more to 6.00%, resulting in one of the lowest inner instabilities among all combinations. The outer ripple attains its minimal point at 0.10%, demonstrating remarkable outer stability. Nonetheless, the mean inner torque decreases further to 20.95 Nm, while the outer torque drops to 3.81 Nm. This blend highlights low ripple percentages while sacrificing torque performance, positioning it as an excellent option for systems where stability is essential.

Inner ripple decreases slightly to 3.55%, indicating excellent inner stability. Outer ripple remains very low at 0.37%, comparable to the outer stability observed in previous combinations. The average inner torque rises dramatically to 21.32 Nm, while the outer torque increases to 35.92 Nm, marking the highest outer torque among all combinations. This combination effectively balances low ripple percentages and high torque performance, making it a well-rounded option for high-performance applications.

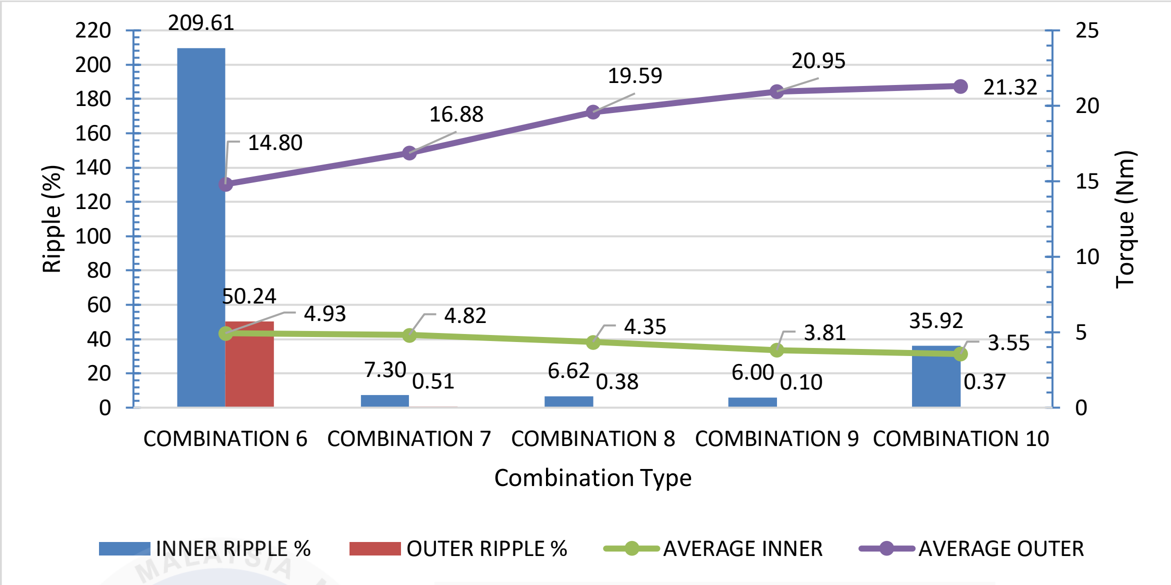

Figure 4.2: Graph Ripple vs Torque for combination 6-10

4.3.3 Graph Ripple vs Torque for Combination 11-15

Combination 11 shows a notable inner ripple percentage of 90.34%, signifying considerable instability in the internal dynamics. The outer ripple percentage stands at 16.51%, indicating a moderate level of instability in the outer area. The typical inner torque is 20.70 Nm, whereas the outer torque is 6.89 Nm, with both indicating satisfactory torque performance despite the elevated ripple percentages. This combination indicates possible inefficiencies in system design or functioning, probably needing modifications to enhance stability.

The inner ripple percentage significantly declines to 18.06%, indicating a remarkable enhancement in inner stability relative to Combination 11. Likewise, the outer ripple percentage dips to 2.08%, indicating a significant decrease in outer instability. The typical inner torque measures 14.95 Nm, whereas the outer torque is 4.27 Nm, suggesting a minor compromise in torque performance for enhanced stability. This arrangement seems to prioritize reducing ripples while balancing stability and moderate torque effectiveness.

Combination 13 lowers the inner ripple percentage to 4.23%, indicating outstanding inner stability. The outer ripple percentage is 0.73%, among the lowest figures, suggesting nearly ideal outer stability. The average inner torque sees a minor rise to 19.07 Nm, while the outer torque stays constant at 0.20 Nm. This blend emphasizes stability with low ripple percentages and could serve as an optimal setup for systems needing reliable performance with diminished variations.

The inner ripple percentage reduces even more to 3.10%, ensuring strong inner stability. Outer ripple remains low at 0.70%, upholding the trend of high external stability. The mean inner torque is 17.10 Nm, indicating a minor decrease, while the outer torque remains at 0.25 Nm, aligning with earlier combinations. This setup achieves minimal ripple percentages while maintaining satisfactory torque output, making it ideal for precision-oriented systems.

Combination 15 demonstrates a minimal inner ripple percentage of 8.78% and an outer ripple percentage of 2.67%, reflecting effectively managed stability in both inner and outer dynamics. The typical inner torque decreases to 16.08 Nm, whereas the outer torque is 0.29 Nm, positioning it among the lowest torque outputs in all combinations. This configuration emphasizes stability while trading off some torque, making it suitable for uses that prioritize reducing ripple rather than maximizing torque output.

UNIVERSITI TEKNIKAL MALAYSIA MELAKA

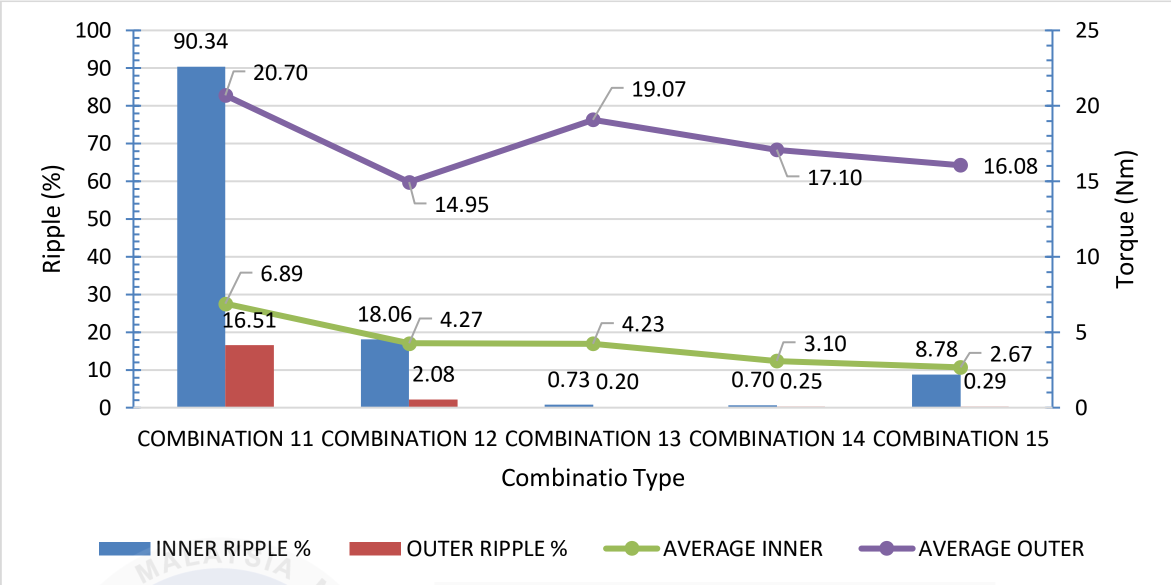

Figure 4.3: Graph Ripple vs Torque for combination 11-15

4.3.4 Graph Ripple vs Torque for Combination 16-20

Combination 16 shows the greatest inner ripple percentage at 195.12%, signifying considerable ripple effects. The percentage of the outer ripple is significant as well, standing at 54.91%, which could result in operational instability or inefficiency. The mean inner torque is recorded at 4.07 Nm, whereas the mean outer torque is comparatively low at 2.01 Nm. This mix signifies inadequate performance caused by high ripple percentages, which may jeopardize the system's longevity and effectiveness.

In Combination 17, there is a significant enhancement in ripple percentages. The percentage of inner ripple declines noticeably to 14.28%, whereas the outer ripple percentage declines steeply to 6.04%. The torque values also enhance, with the mean inner torque climbing to 4.08 Nm and the mean outer torque reaching 4.49 Nm. This mix shows an improved equilibrium between ripple minimization and torque efficiency, rendering it more appropriate for real-world uses.

In Combination 18, the inner ripple percentage keeps decreasing to 15.02%, whereas the outer ripple percentage stays stable at 3.47%, a figure that is quite low. The typical inner torque diminishes modestly to 3.29 Nm, while the average outer torque increases to 9.09 Nm. This combination demonstrates moderate ripple suppression while attaining a substantial boost in outer torque, potentially making it more suitable for applications that demand higher torque output.

Combination 19 demonstrates an additional decrease in ripple effects. The inner ripple percentage decreases to 16.03%, while the outer ripple percentage stays low at 2.91%. The typical inner torque decreases slightly to 2.51 Nm, while the typical outer torque reaches a peak of 16.03 Nm, which is the highest of all combinations. This blend is very successful for situations that emphasize peak torque delivery with regulated ripple rates.

Combination 20 reaches the lowest inner ripple percentage of 2.60% and a minimal outer ripple percentage of 0.60%, demonstrating outstanding ripple suppression. Nevertheless, the mean inner torque falls to 2.28 Nm, while the average outer torque plummets to 7.64 Nm, indicating a compromise between torque and ripple mitigation. This blend is ideal for scenarios where reducing ripple is more important than obtaining high torque.

UNIVERSITI TEKNIKAL MALAYSIA MELAKA

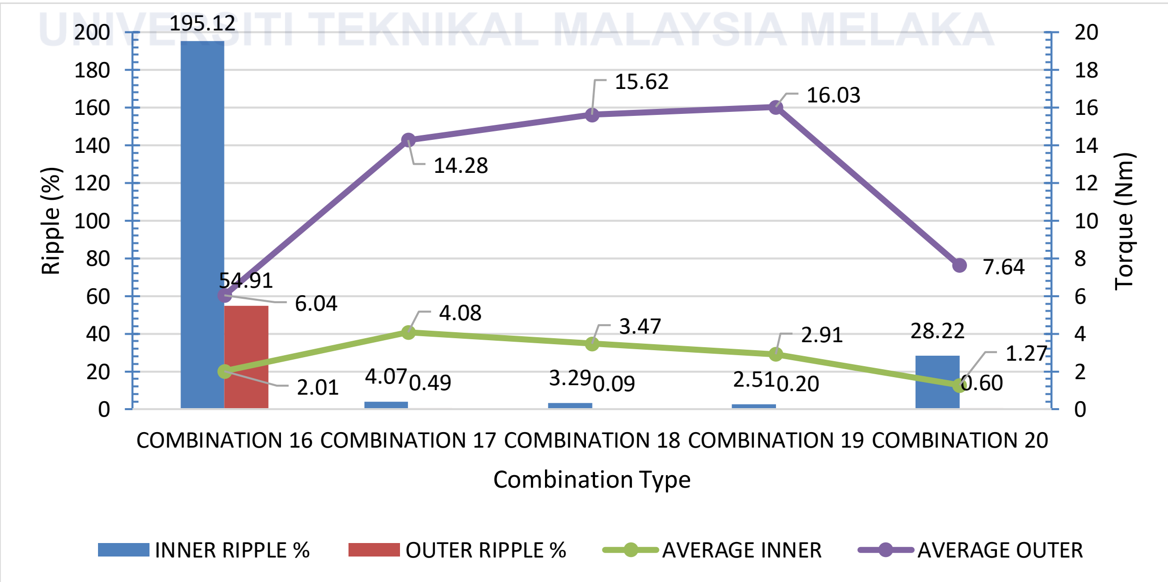

Figure 4.4: Graph Ripple vs Torque for combination 16-20

4.3.5 Graph Time vs Torque for Combination 14

Figure 4.5 illustrates the graph for Combination 14, showing the torque behavior over time for the Ni (Inner) and No (Outer) conditions. From the graph, it can be observed that the torque for Ni (blue line) remains constant at 3 Nm, representing the best result as it is the lowest torque compared to other combination graphs. Similarly, the torque for No (orange line) steadily increases to approximately 17 Nm, which is also the lowest torque for No when compared to other combinations.

Under both conditions, the torque remains stable and consistent over time, with no significant oscillations or fluctuations, demonstrating the system's stability and reliability. Based on these results, Combination 14 delivers the best performance among all combinations, as it achieves the lowest torque values for both Ni and No while maintaining a straight and consistent graph. This reflects the system's efficiency and overall stability.

UNIVERSITI TEKNIKAL MALAYSIA MELAKA

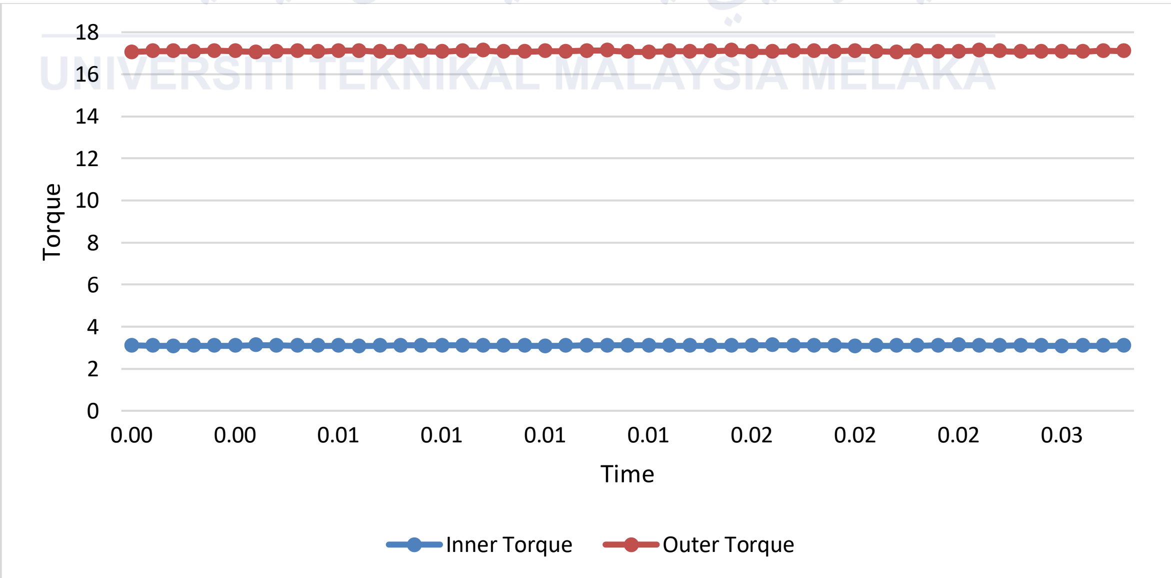

Figure 4.5: Time vs Torque for Combination 14

4.4 Result Summary

The computed findings show a strong correlation between the gear ratio and the number of outer pole pairs. Before running the JMAG simulation, the gear ratios for different configurations were calculated using Equation 14. To verify correctness, these computed ratios were then contrasted with the outcomes of the simulation. There was a clear association between these two factors, as evidenced by the observation that the gear ratio grew along with the number of outer pole pairs. The significance of modifying the number of outer pole pairs to get the intended gear ratio is highlighted by this discovery, which is critical for optimising gear design.

Table 4.2: Torque ripple and average for all combination

LABEL	INNER RIPPLE %	AVERAGE INNER	OUTER RIPPLE %	AVERAGE OUTER
COMBINATION 1	111.65	9.53	18.41	28.60
COMBINATION 2	2.74	8.37	0.08	29.31
COMBINATION 3	40.13	6.14	10.22	27.82
COMBINATION 4	1.82	5.12	0.08	28.21
COMBINATION 5	48.33	4.43	10.22	26.85
COMBINATION 6	209.61	4.93	50.24	14.80
COMBINATION 7	7.30	4.82	0.51	16.88
COMBINATION 8	6.62	4.35	0.38	19.59
COMBINATION 9	6.00	3.81	0.10	20.95
COMBINATION 10	35.92	3.55	0.37	21.32
COMBINATION 11	90.34	6.89	16.51	20.70
COMBINATION 12	18.06	4.27	2.08	14.95
COMBINATION 13	0.73	4.23	0.20	19.07
COMBINATION 14	0.70	3.10	0.25	17.10
COMBINATION 15	8.78	2.67	0.29	16.08
COMBINATION 16	195.12	2.01	54.91	6.04
COMBINATION 17	4.07	4.08	0.49	14.28
COMBINATION 18	3.29	3.47	0.09	15.62
COMBINATION 19	2.51	2.91	0.20	16.03
COMBINATION 20	28.22	1.27	0.60	7.64

CHAPTER 5

CONCLUSION AND RECOMMENDATIONS

5.1 Conclusion

In conclusion, the design phase involved creating several models of magnetic gear structures using flux modulation principles, focusing on 20 combination designs based on different pole pair combinations. These designs were carefully developed to ensure a diverse range of configurations that could effectively explore the potential performance characteristics of magnetic gears under varying conditions. This approach allowed for a systematic investigation into the relationship between pole pair combinations and gear performance.

Subsequently, a comprehensive evaluation of the torque behavior of Concentric Magnetic Gears was conducted using the Finite Element Method (FEM). This method provided precise and detailed data, offering insights into key torque characteristics, including torque ripple and average torque, for each of the 20 combination designs. The evaluation highlighted the differences in performance across the configurations, enabling the identification of trends and factors influencing torque behavior.

Finally, the results were systematically compared across all combinations to determine the configurations that produced the lowest torque ripple and the highest average torque. This analysis not only identified the optimal pole pair combination with superior performance metrics but also demonstrated the importance of balancing torque stability and efficiency. These findings offer valuable insights for future developments in magnetic gear design, emphasizing the critical role of selecting the appropriate pole pair combination to achieve enhanced performance and reliability.

5.2 Future Works

For future studies, it is recommended to explore material optimization, considering the impact of different materials on CMG performance. Additionally, investigating temperature effects, dynamic load analysis, and validation through prototyping can contribute to a more comprehensive understanding of CMG behavior. Exploring integration with electric vehicles, employing advanced simulation techniques, conducting parametric studies, and assessing fault tolerance and reliability are crucial aspects that merit attention in further research. By addressing these areas, future studies can enhance the applicability and performance of Concentric Magnetic Gears, particularly in the context of electric vehicles and other high performance systems.

5.3 Potential for Commercialization

This project presents significant potential for commercialization, particularly in industries focusing on electric vehicles (EVs), renewable energy systems, and industrial automation. With the global EV market rapidly expanding due to the shift toward sustainable transportation, the optimization of magnetic gears for reduced torque ripple and enhanced energy efficiency directly addresses the demand for high-performance, cost-effective drivetrain solutions. By integrating the findings of this research, EV manufacturers can reduce energy consumption, improve vehicle range, and enhance overall performance, thereby gaining a competitive edge in the market.

Beyond EVs, magnetic gears with optimized torque behavior have broad industrial applications, including robotics, wind energy, and automation, offering benefits such as lower maintenance requirements, reduced noise, and improved efficiency. The alignment of this research with Sustainable Development Goals (SDGs) 7 (Affordable and Clean Energy) and 9 (Industry, Innovation, and Infrastructure) further enhances its appeal to governments

UNIVERSITI TEKNIKAL MALAYSIA MELAKA

and organizations prioritizing sustainability and environmental compliance. Additionally, the innovative use of JMAG software ensures precision and scalability, making these magnetic gears attractive to manufacturers seeking advanced torque management solutions.

The commercialization potential is also strengthened by opportunities for intellectual property protection through patents and proprietary methodologies, enabling licensing agreements or collaborations with EV manufacturers and gear producers. Moreover, magnetic gears' inherent advantages, such as reduced maintenance costs and extended lifespans, offer a compelling value proposition for cost-sensitive markets. By addressing critical performance gaps in EVs and other industries, this project provides a transformative solution with broad commercial applicability, fostering sustainable growth and technological innovation.

UNIVERSITI TEKNIKAL MALAYSIA MELAKA

REFERENCES

[1] P. M. Tlali, R. J. Wang, and S. Gerber, "Magnetic gear technologies: A review," in *Proceedings - 2014 International Conference on Electrical Machines, ICEM 2014*, Institute of Electrical and Electronics Engineers Inc., Nov. 2020, pp. 544–550. doi: 10.1109/ICELMACH.2014.6960233.

[2] B. McGilton, R. Crozier, A. McDonald, and M. Mueller, "Review of magnetic gear technologies and their applications in marine energy," in *IET Renewable Power Generation*, Institution of Engineering and Technology, 2019, pp. 174–181. doi: 10.1049/iet-rpg.2017.0210.

[3] G. Ruiz-Ponce, M. A. Arjona, C. Hernandez, and R. Escarela-Perez, "A Review of Magnetic Gear Technologies Used in Mechanical Power Transmission," Feb. 01, 2023, *MDPI*. doi: 10.3390/en16041721.

[4] A. Al Faysal and S. Mohamed Haris, "Development of Magnetic Gears: A Review," *Jurnal Kejuruteraan*, vol. si1, no. 7, pp. 49–56, Nov. 2021, doi: 10.17576/jkukm-2018-si1(7)-06.

[5] M. Fikrie and B. Ridwan, "AN EVALUATION OF TORQUE BEHAVIOUR OF CONCENTRIX MAGNETIC GEAR (CMG)USING FINITE ELEMENT METHOD (FEM) FOR ELECTRIC VEHICLE APPLICATION," 2023.

[6] L. Dimauro *et al.*, "Magnetic gearbox for automotive power transmissions: An innovative industrial technology," *Engineering Science and Technology, an International Journal*, vol. 46, Oct. 2023, doi: 10.1016/j.jestch.2023.101497.

[7] A. Ferreira Flores Filho, D. Luciano Figueiredo, A. Santos Nunes, C. G. C Neves, and Á. Ferreira Flores, "Magnetic Gear: A Review," 2019, doi: 10.13140/RG.2.1.1689.2326.

[8] A. Shoaei and Q. Wang, "A Comprehensive Review of Concentric Magnetic Gears," *IEEE Transactions on Transportation Electrification*, 2023, doi: 10.1109/TTE.2023.3317772.

[9] L. Jing, J. Gong, Z. Huang, T. Ben, and Y. Huang, "A New Structure for the Magnetic Gear," *IEEE Access*, vol. 7, pp. 75550–75555, 2019, doi: 10.1109/ACCESS.2019.2919679.

[10] M. Firdaus *et al.*, "A New Speed Multiplier Coaxial Magnetic Gear," 2020.

UNIVERSITI TEKNIKAL MALAYSIA MELAKA

[11] C. Tan, W. Liu, Y. Rao, W. Tang, and L. Jing, “Loss Analysis of Magnetic Gear with Slotted in Magnetic Modulation Ring,” *CES Transactions on Electrical Machines and Systems*, vol. 7, no. 1, pp. 110–117, 2023, doi: 10.30941/CESTEMS.2023.00001.

[12] M. Desvaux *et al.*, “Gear ratio optimization of a full magnetic indirect drive chain for wind turbine applications ratio optimization of a full magnetic indirect drive chain for wind turbine applications,” pp. 1–9, 2018, doi: 10.1109/EVER.2017.7935894ï.

[13] K. Stierstadt and M. Liu, “Maxwell’s stress tensor and the forces in magnetic liquids,” *ZAMM Zeitschrift fur Angewandte Mathematik und Mechanik*, vol. 95, no. 1, pp. 4–37, Jan. 2019, doi: 10.1002/zamm.201300192.

[14] M. F. M. Ab Halim, “Preliminary Magnetization Pattern Study on Magnetic Gear,” *International Journal of Advanced Trends in Computer Science and Engineering*, vol. 9, no. 3, pp. 4063–4067, Jun. 2020, doi: 10.30534/ijatcse/2020/233932020.

[15] N. Misron, L. M. Saini, I. Aris, C. A. Vaithilingam, and H. Tsuyoshi, “Simplified design of magnetic gear by considering the maximum transmission torque line,” *Applied Sciences (Switzerland)*, vol. 10, no. 23, pp. 1–14, Dec. 2020, doi: 10.3390/app10238581.

[16] B. McGilton, R. Crozier, and M. Mueller, “Optimisation procedure for designing a magnetic gear,” *The Journal of Engineering*, vol. 2017, no. 13, pp. 840–843, Jan. 2019, doi: 10.1049/joe.2017.0448.

[17] G. Galmadi and D. Galmadi, “Analysis of Some Design Parameters and Constructive Solutions for Coaxial Magnetic Gears,” *Bulletin of the Polytechnic Institute of Iași. Machine constructions Section*, vol. 69, no. 2, pp. 95–108, Jun. 2023, doi: 10.2478/bipcm-2023-0018.

[18] G. Muruganandam, S. Padma, and P. Selvakumar, “Torque Analysis of Magnetic Spur Gear with Different Configurations,” 2022. [Online]. Available: http://www.irphouse.com

[19] M. Desvaux, R. Le Goff Latimier, B. Multon, H. Ben Ahmed, and S. Sire, “Design and Optimization of Magnetic Gears with Arrangement and Mechanical Constraints for Wind Turbine Applications. EVER’16,” EVER, 2022. [Online]. Available: https://hal.science/hal-01312302

UNIVERSITI TEKNIKAL MALAYSIA MELAKA

[20] E. Marcin Kowol, J. Kołodziej, and M. Łukaniszyn, "CZASOPISMO TECHNICZNE AN ANALYSIS OF MAGNETIC GEAR PERFORMANCE ANALIZA PRACY PRZEKŁADNI MAGNETYCZNEJ," 2019, doi: 10.4467/2353737XCT.15.030.3830.

[21] M. Filippini Supervisor, P. Alotto Coordinator, and R. Turri, "Magnetic gears numerical modelling and optimization," 2022.

[22] S. Gerber, "Evaluation and Design Aspects of Magnetic Gears and Magnetically Geared Electrical Machines," 2021. [Online]. Available: https://scholar.sun.ac.za

[23] "Review and Analysis of Coaxial Magnetic Gear," 2020.

[24] M. Hafiz, A. Azhar, and E. Sulaiman, "Design and Analysis of Concentric Magnetic Gear for Speed Enhancer," *Evolution in Electrical and Electronic Engineering*, vol. 3, no. 2, pp. 400–410, 2022, doi: 10.30880/eeee.2022.03.02.047.

[25] M. F. M. Ab Halim, A. Ab Rahman, M. S. Yahaya, and E. Sulaiman, "Hybrid-excited magnetic gear topology for improved gear efficiency at increasing rotor speed," *International Journal of Power Electronics and Drive Systems*, vol. 15, no. 1, pp. 91–97, Mar. 2024, doi: 10.11591/ijpeds.v15.i1.pp91-97.

اونيۏرسيتي تيكنيكل مليسيا ملاك
UNIVERSITI TEKNIKAL MALAYSIA MELAKA

APPENDICES

Appendix 1

Combination 1:

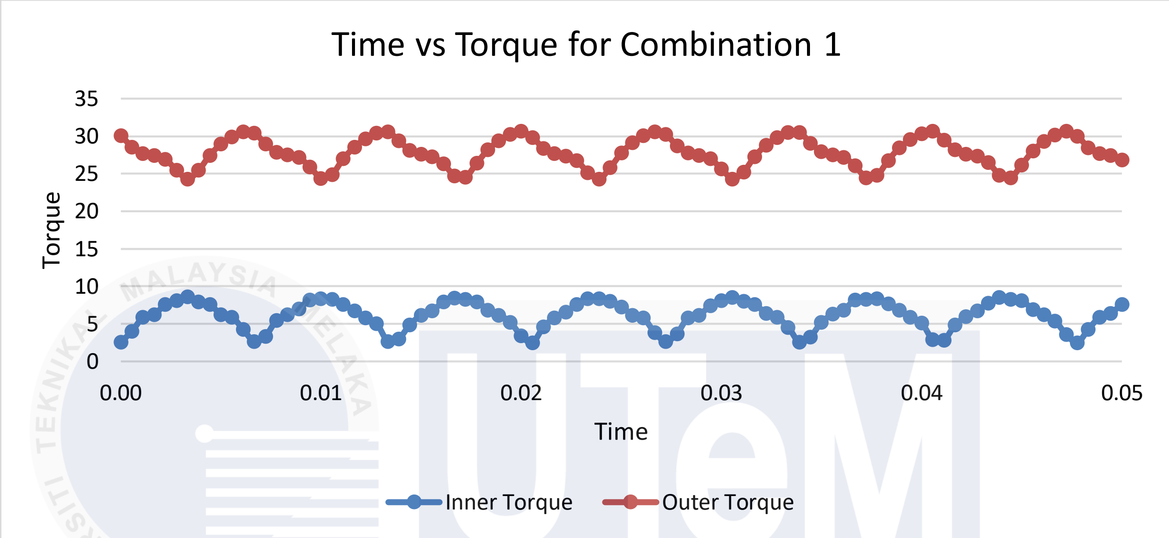

Integral Average	-6.138499231	-27.81899748
RATIO	4.531889056	
MIN	-8.601943983	-30.66186443
DIFF MAX & MIN	2.463444752	2.842866945
RIPPLE%	40.13105907	10.2191567

UNIVERSITI TEKNIKAL MALAYSIA MELAKA

Combination 2:

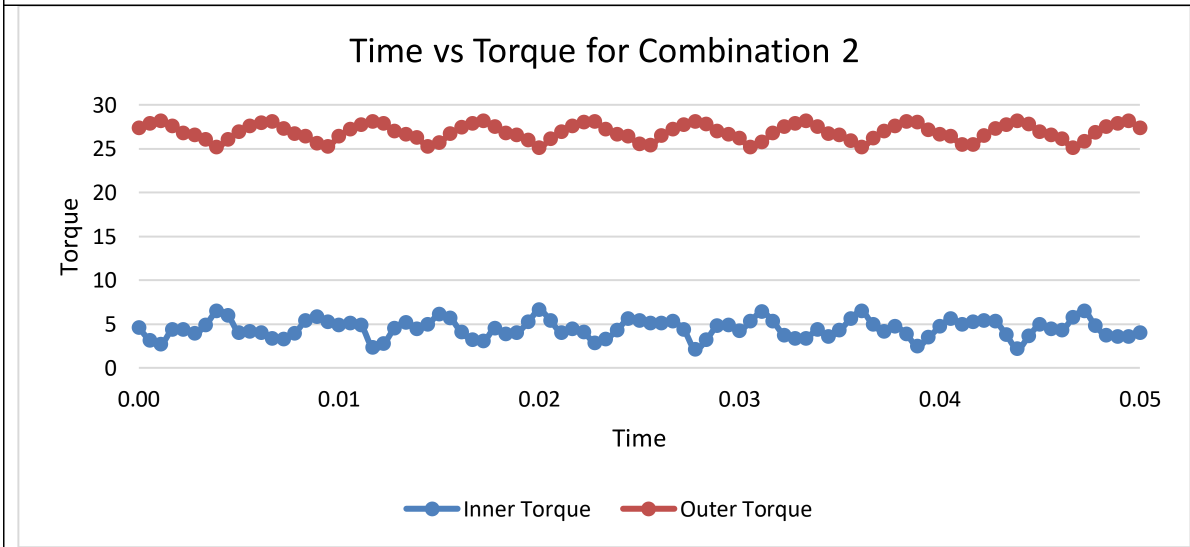

Integral Average	-4.432101011	-26.84509607
RATIO	6.056968469	
MIN	-6.574012674	-28.17533556
DIFF MAX&MIN	2.141911663	1.330239486
RIPPLE%	48.32723031	4.955242039

Combination 3:

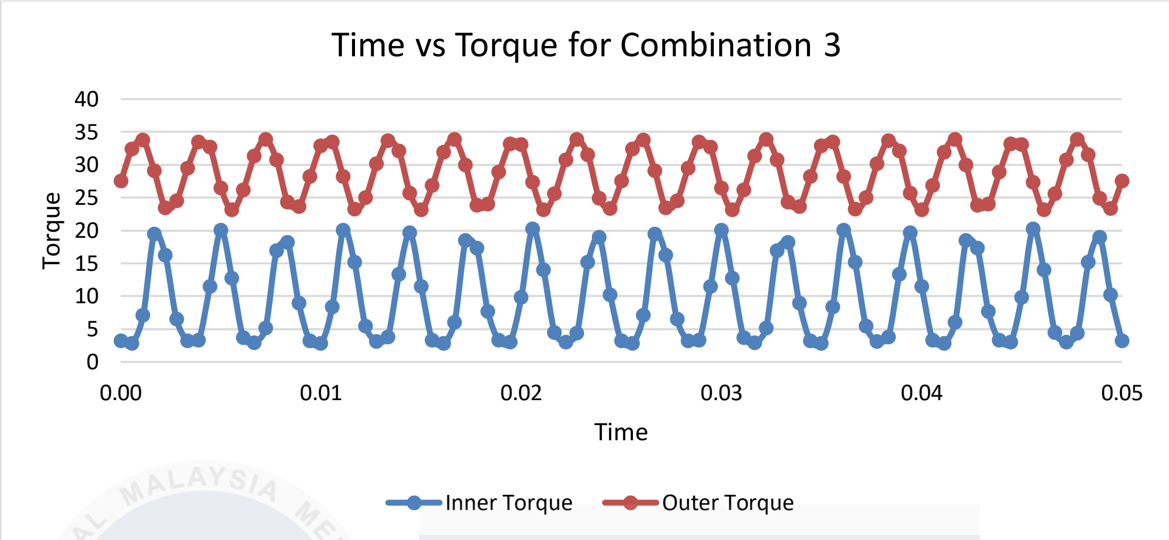

Integral Average	-9.529537618	-28.59506331
RATIO	3.00067689	
MIN	-20.16971244	-33.8589035
DIFF MAX & MIN	10.64017482	5.263840197
RIPPLE %	111.6546809	18.40821312

Combination 4:

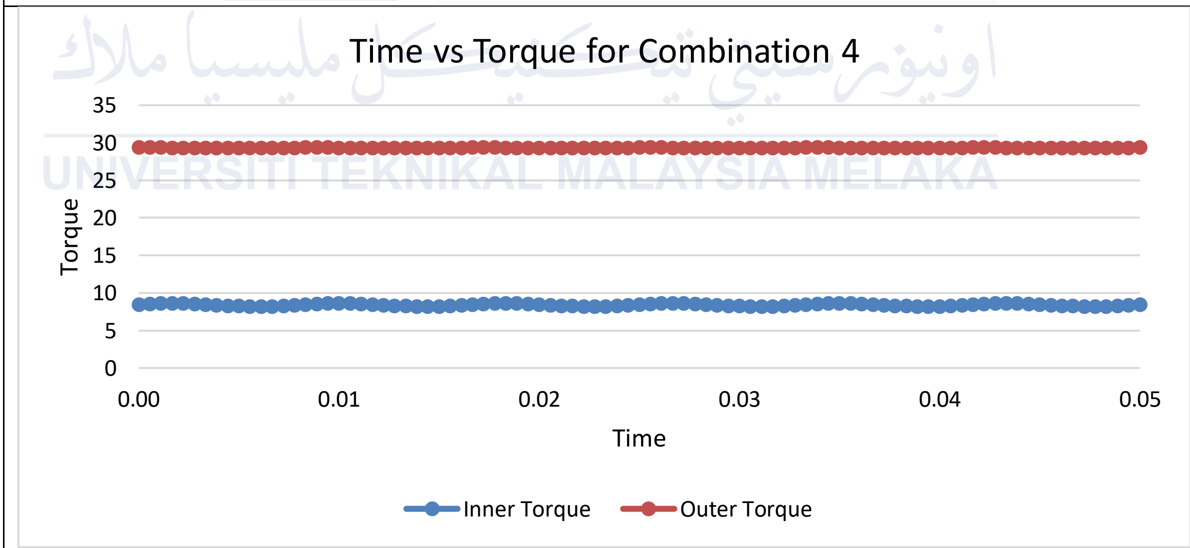

Integral Average	-8.37193994	-29.31126198
RATION	3.501131422	
MIN	-8.601272992	-29.33552701
DIFF MAX & MIN	0.229333052	0.02426503
RIPPLE %	2.739305985	0.082783984

Combination 5:

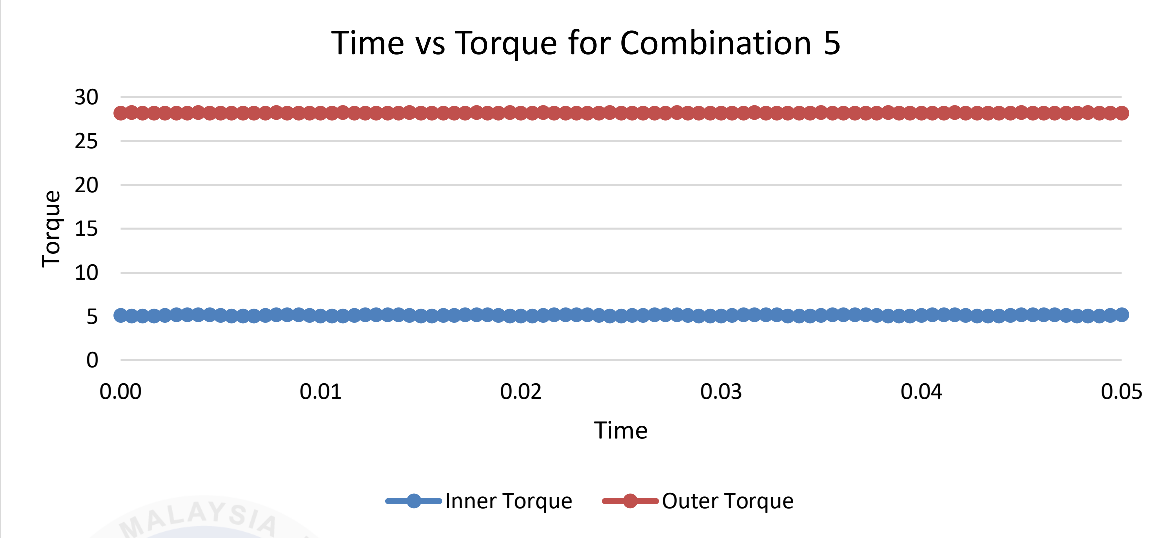

Integral Average	-5.123232524	-28.21336432
RATIO	5.506945895	
MIN	-5.216665657	-28.23474842
DIFF MAX & MIN	0.093433133	0.021384101
RIPPLE%	1.823714482	0.075794225

Combination 6:

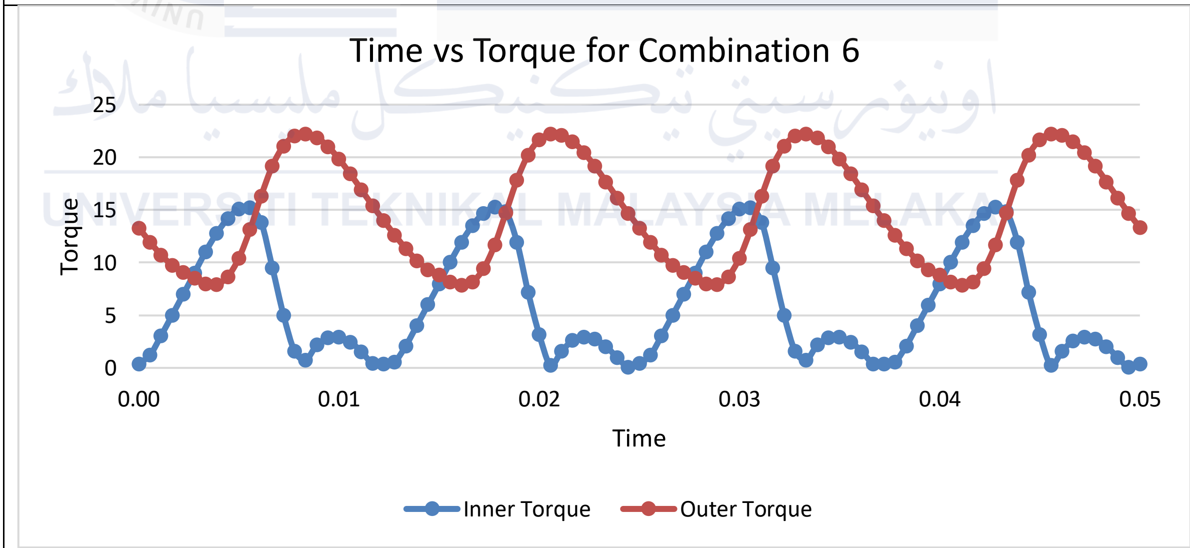

Integral Average	-4.934000642	-14.80372508
RATIO	3.000349241	
MIN	-15.27601292	-22.24084011
DIFF MAX & MIN	10.34201228	7.437115027
RIPPLE%	209.6070314	50.23813253

Combination 7:

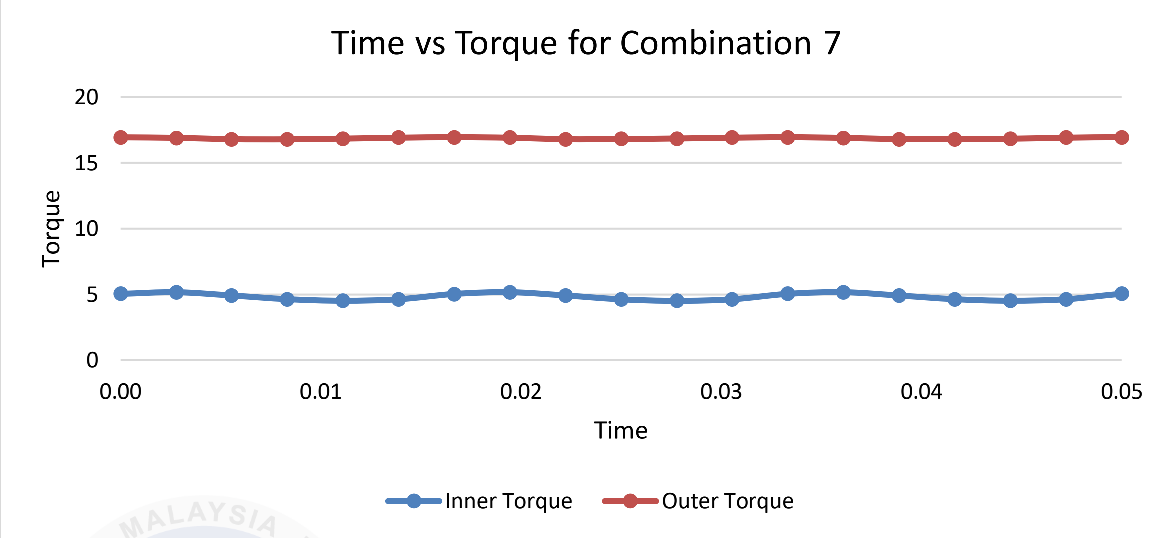

Integral Average	-4.820593706	-16.87577301
RATIO	3.500766511	
MIN	-5.172346366	-16.96205722
DIFF MAX & MIN	0.35175266	0.086284214
RIPPLE%	7.296874238	0.51129044

Combination 8:

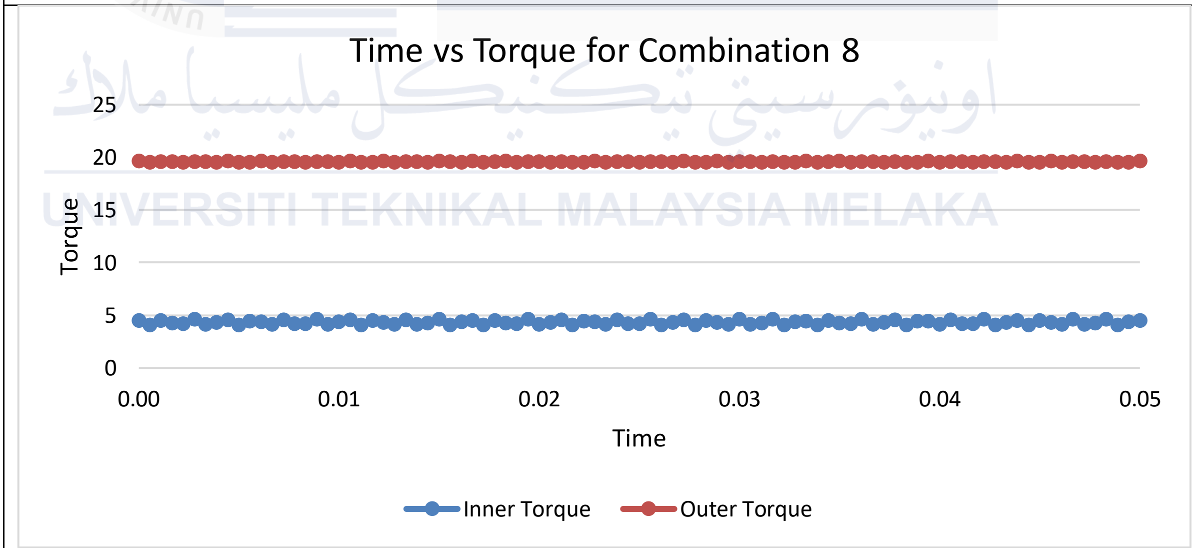

Integral Average	-4.352377746	-19.58771983
RATIO	4.500464108	
MIN	-4.6403387	-19.66118233
DIFF MAX & MIN	0.287960954	0.073462501
RIPPLE%	6.61617559	0.375043658

Combination 9:

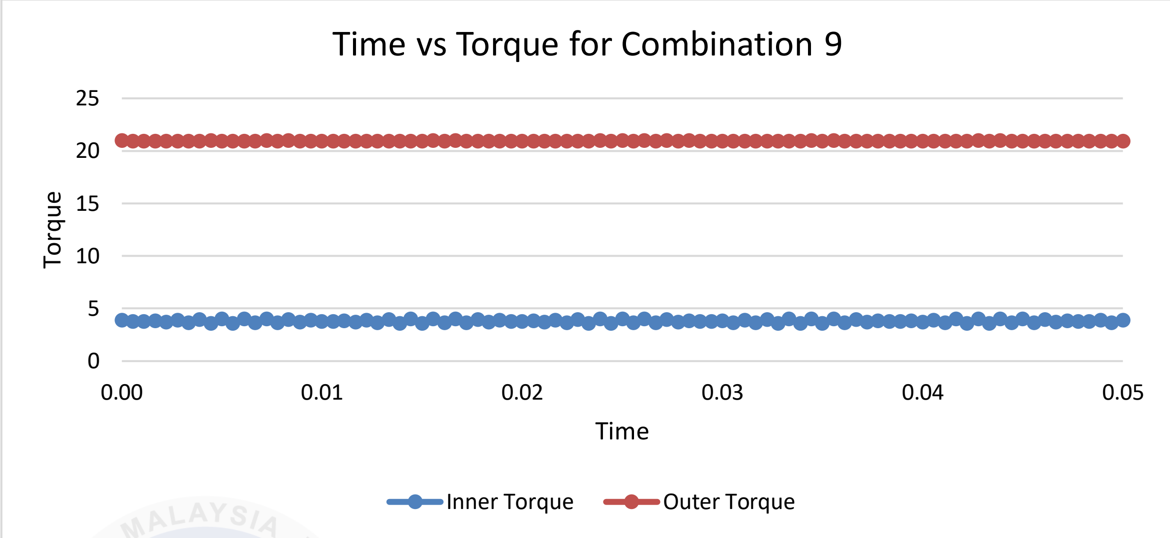

Integral Average	-3.807911082	-20.95276724
RATIO	5.502430806	
MIN	-4.036385331	-20.9747569
DIFF MAX & MIN	0.228474249	0.021989661
RIPPLE%	5.99998909	0.104948718

Combination 10:

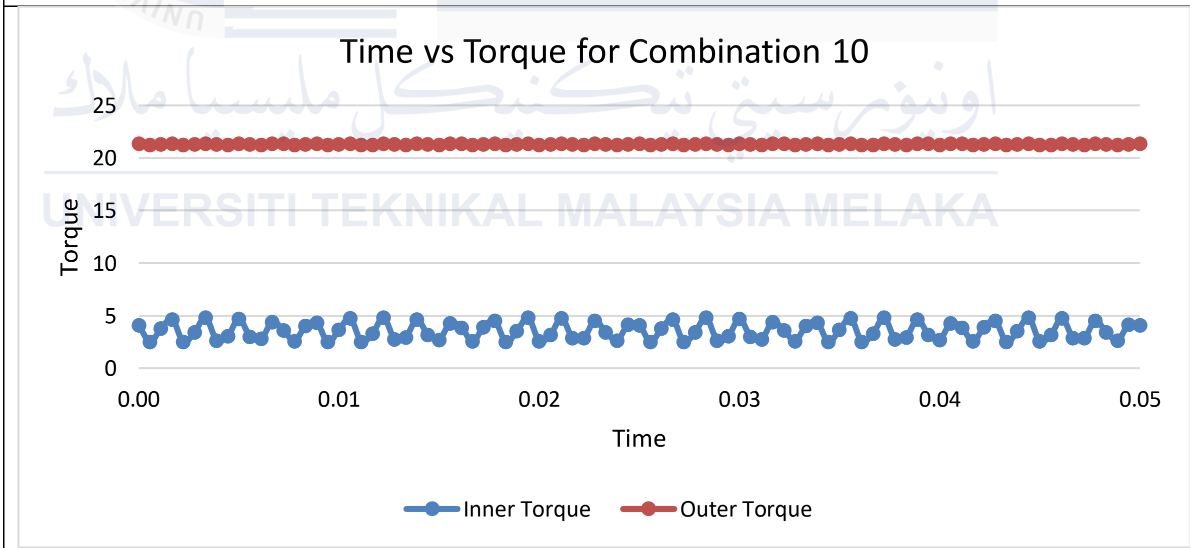

Integral Average	-3.551460758	-21.3165973
RATIO	6.002205503	
MIN	-4.827140465	-21.39641122
DIFF MAX & MIN	1.275679707	0.079813912
RIPPLE%	35.9198593	0.374421445

UNIVERSITI TEKNIKAL MALAYSIA MELAKA

Combination 11:

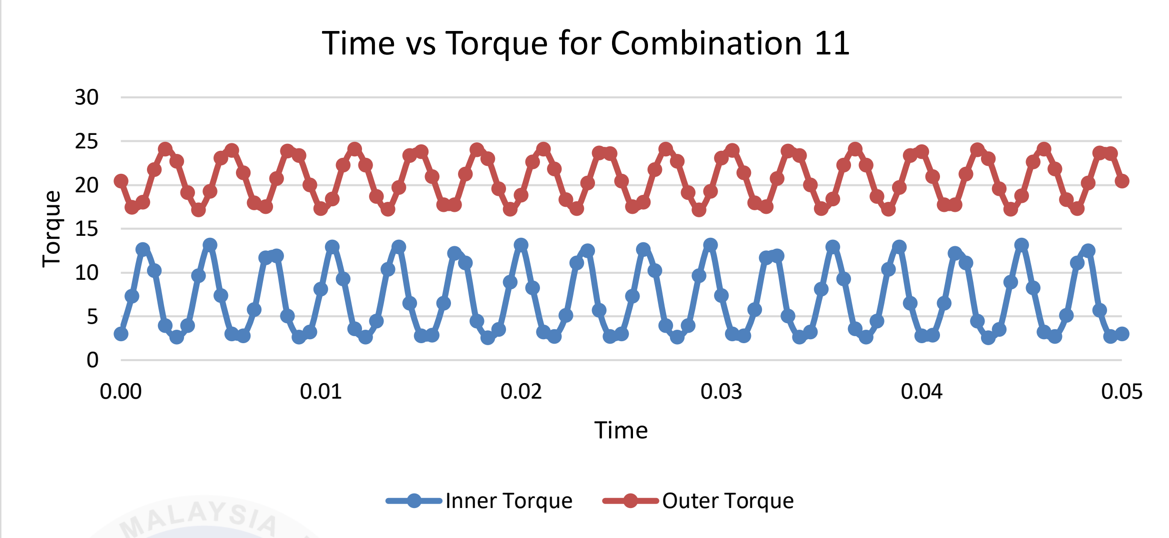

Integral Average	-6.892930433	-20.69509404
RATIO	3.002365139	
MIN	-13.11995563	-24.11082594
DIFF MAX & MIN	6.227025199	3.415731905
RIPPLE%	90.33930141	16.50503206

Combination 12:

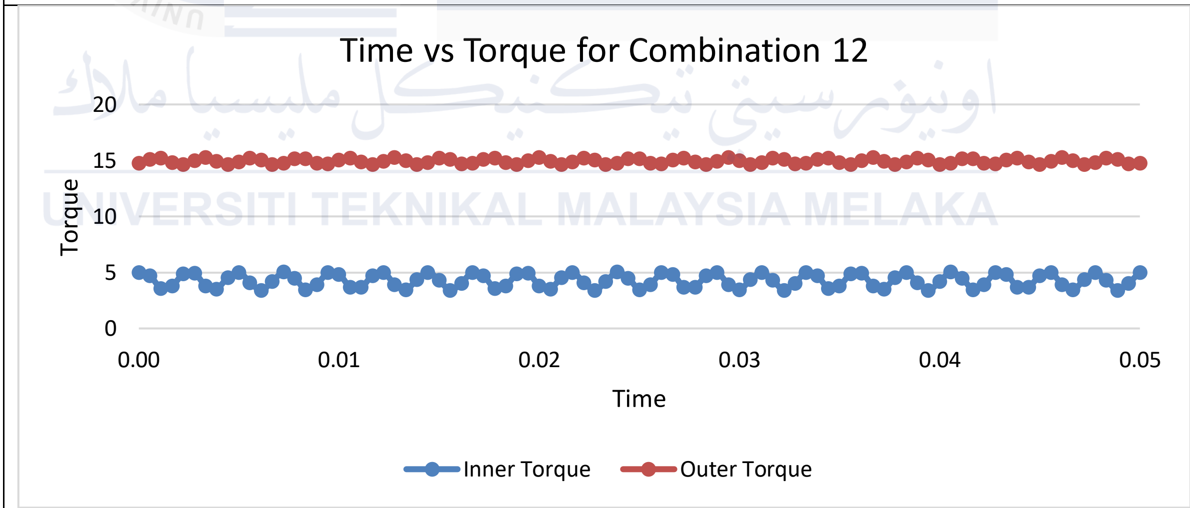

Integral Average	-4.26629862	-14.94796107
RATIO	3.50373061	
MIN	-5.036722763	-15.25856451
DIFF MAX & MIN	0.770424143	0.310603445
RIPPLE%	18.05837358	2.077898409

Combination 13:

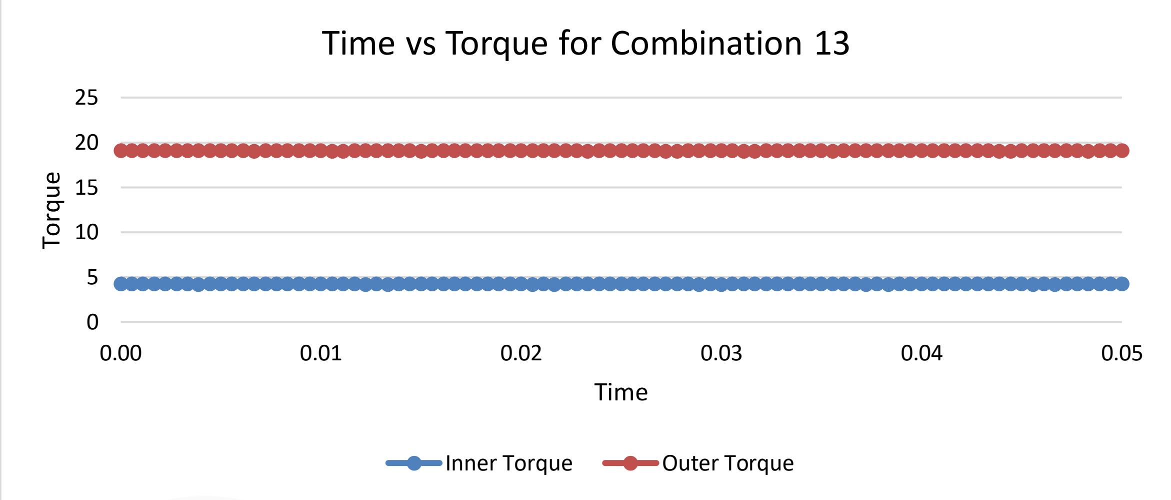

Integral Average	-4.23097598	-19.07374004
RATIO	4.508118251	
MIN	-4.261815852	-19.11112045
DIFF MAX & MIN	0.030839872	0.037380419
RIPPLE%	0.728906804	0.195978444

Combination 14:

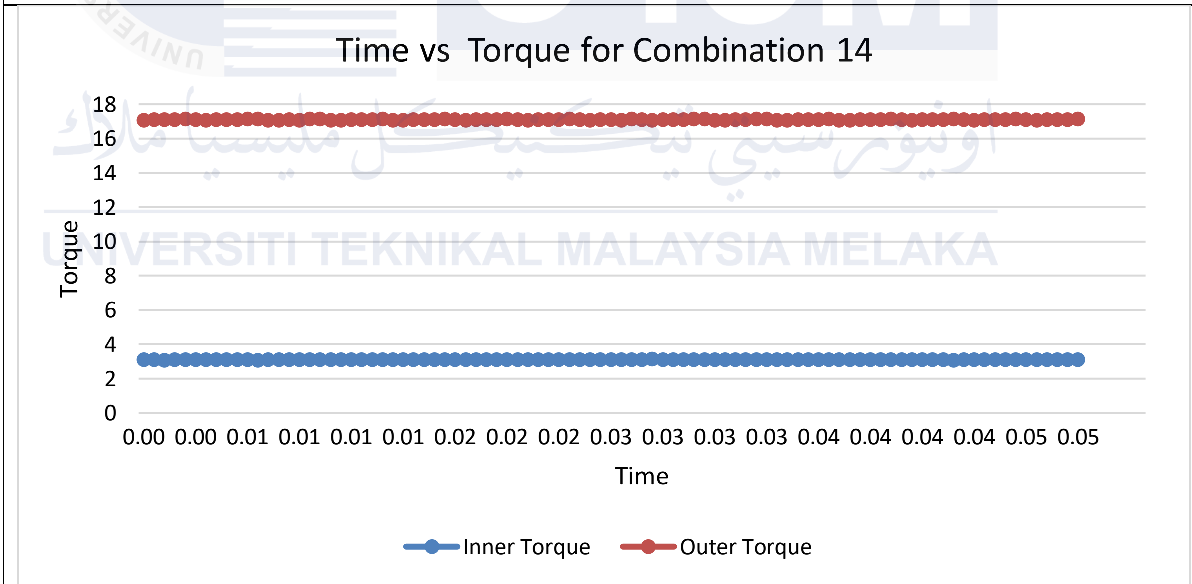

Integral Average	-3.099473268	-17.09575382
RATIO	5.515696487	
MIN	-3.121318764	-17.13782581
DIFF MAX & MIN	0.021845496	0.042071995
RIPPLE%	0.704813169	0.246096167

Combination 15:

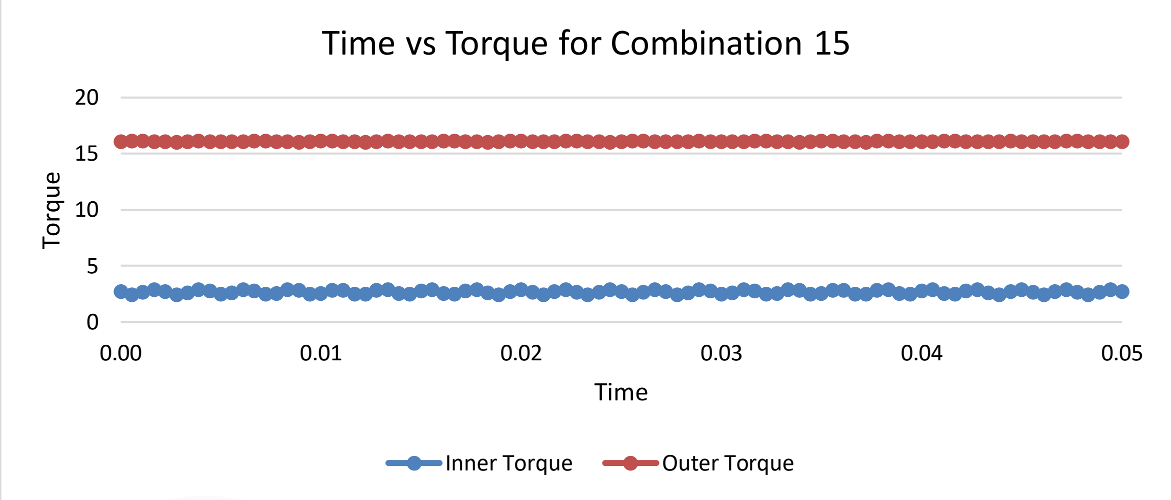

Integral Average	-2.670556484	-16.075998
RATIO	6.019718401	
MIN	-2.905102134	-16.12219988
DIFF MAX & MIN	0.23454565	0.046201872
RIPPLE%	8.782650789	0.287396604

Combination 16:

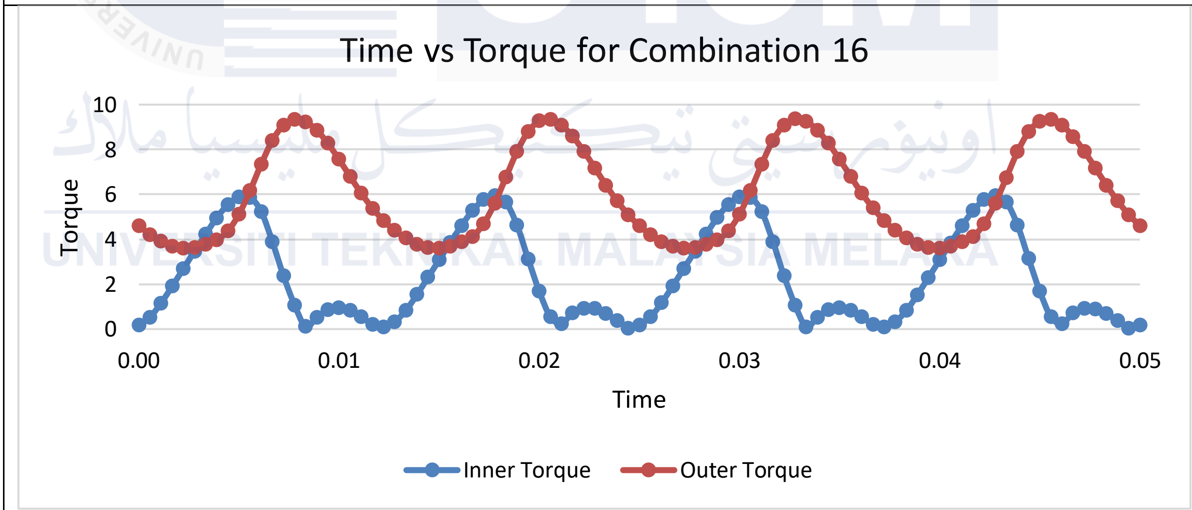

Integral Average	-2.012090207	-6.038071507
RATIO	3.000895033	
MIN	-5.938127556	-9.353805511
DIFF MAX & MIN	3.926037349	3.315734004
RIPPLE%	195.1223327	54.91379159

Combination 17:

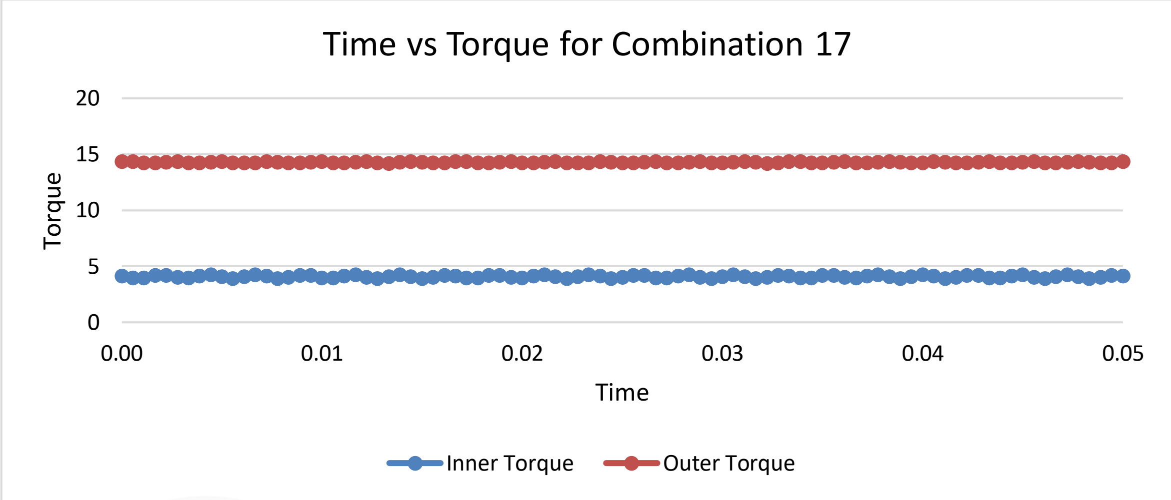

Integral Average	-4.077612592	-14.27820786
RATIO	3.501609713	
MIN	-4.243461308	-14.34813885
DIFF MAX & MIN	0.165848716	0.06993099
RIPPLE%	4.067299487	0.489774281

Combination 18:

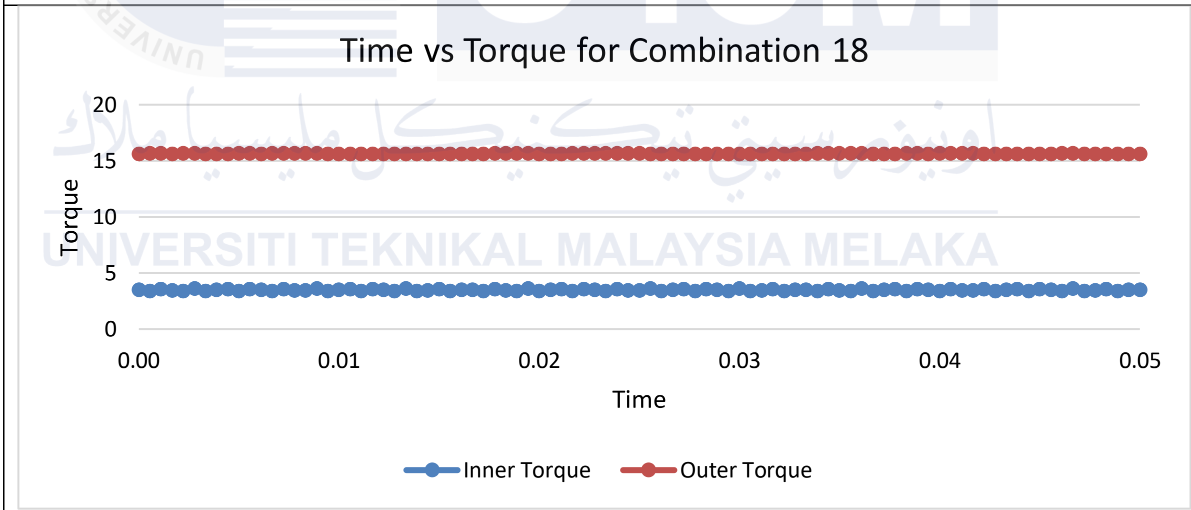

Integral Average	-3.469290794	-15.62177698
RATIO	4.502873326	
MIN	-3.583478487	-15.63579716
DIFF MAX & MIN	0.114187693	0.014020177
RIPPLE%	3.291384308	0.089747647

UNIVERSITI TEKNIKAL MALAYSIA MELAKA

Combination 19:

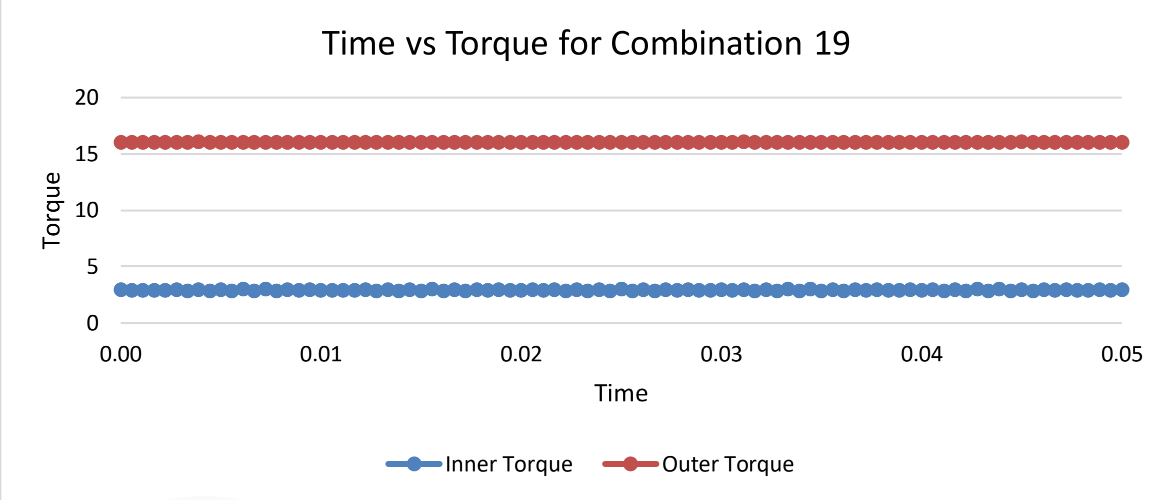

Integral Average	-2.912381178	-16.03297949
RATIO	5.505110254	
MIN	-2.985463941	-16.06473899
DIFF MAX & MIN	0.073082762	0.031759496
RIPPLE%	2.509381766	0.198088549

Combination 20:

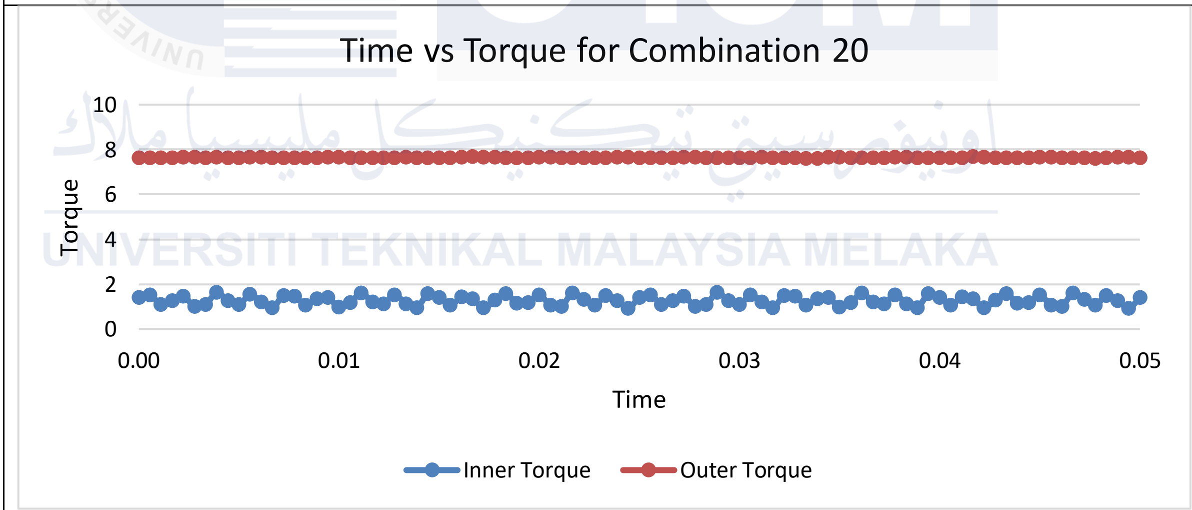

Integral Average	-1.271430685	-7.635685132
RATIO	6.005585065	
MIN	-1.630210288	-7.681380238
DIFF MAX & MIN	0.358779603	0.045695106
RIPPLE%	28.21857359	0.598441468

UNIVERSITI TEKNIKAL MALAYSIA MELAKA

GANTT CHART

Task	WEEK													
	01	02	03	04	05	06	07	08	09	10	11	12	13	14
Adding news design														
Determine number of pole pair on each design														
Completing all design														
Collect data from each design														
Submit logbook														
Get the data and result														
Organize and analysis data														
Report and documentation														
Submit report to supervisor														
Submit report to panel														
Presentation														
Project completion														
Submit to E-Thesis														

UNIVERSITI TEKNIKAL MALAYSIA MELAKA